

**LABORATORY DETERMINATION OF MECHANICAL
AND HYDRAULIC PROPERTIES OF CONSOLIDATED
SLUDGE-CRUSHED SALT MIXTURES FOR
BACKFILLING IN SALT AND
POTASH MINES**



**A Thesis Submitted in Partial Fulfillment of the Requirements for the
Degree of Master of Engineering in Geotechnology
Suranaree University of Technology
Academic Year 2015**

การทดสอบคุณสมบัติเชิงกลศาสตร์และเชิงพลศาสตร์ของดินตะกอนประปา
ผสมกับเกลือบดภายใต้การบดอัด เพื่อถมกลับใน
เหมืองเกลือหินและเหมืองโพแทช



วิทยานิพนธ์นี้เป็นส่วนหนึ่งของการศึกษาตามหลักสูตรปริญญาวิศวกรรมศาสตรมหาบัณฑิต
สาขาวิชาเทคโนโลยีธรณี
มหาวิทยาลัยเทคโนโลยีสุรนารี
ปีการศึกษา 2558

**LABORATORY DETERMINATION OF MECHANICAL AND
HYDRAULIC PROPERTIES OF CONSOLIDATED SLUDGE-
CRUSHED SALT MIXTURES FOR BACKFILLING
IN SALT AND POTASH MINES**

Suranaree University of Technology has approved this thesis submitted in
partial fulfillment of the requirements for a Master's Degree.

Thesis Examining Committee

(Asst. Prof. Dr. Decho Phueakphum)

Chairperson

(Dr. Prachya Tepnarong)

Member (Thesis Advisor)

(Prof. Dr. Kittitep Fuenkajorn)

Member

(Prof. Dr. Sukit Limpijumnong)

Vice Rector for Academic Affairs
and Innovation

(Assoc. Prof. Flt. Lt. Dr. Kontorn Chamniprasart)

Dean of Institute of Engineering

อดิศร บำรุงสุข : การทดสอบคุณสมบัติเชิงกลศาสตร์และเชิงชลศาสตร์ของดินตะกอน
ประปาผสมกับเกลือบดภายใต้การบดอัดเพื่อถมกลับในเหมืองเกลือหินและเหมือง โพแทช
(LABORATORY DETERMINATION OF MECHANICAL AND HYDRAULIC
PROPERTIES OF CONSOLIDATED SLUDGE-CRUSHED SALT MIXTURE FOR
BACKFILLING IN SALT AND POTASH MINES) อาจารย์ที่ปรึกษา : อาจารย์ ดร.
ปรัชญา เทพนรงค์, 114 หน้า.

วัตถุประสงค์ของการศึกษานี้คือเพื่อศึกษาค่ากำลังรับแรงและค่าซึมผ่านของส่วนผสมดิน
ตะกอนประปากับเกลือบดภายใต้ผลกระทบของความเค็มและระยะเวลาการอัดตัวคายน้ำ
อัตราส่วนของตะกอนประปาผสมกับเกลือบดผันแปรจาก 0:100, 25:75, 50:50, 75:25 ถึง 100:0 โดย
น้ำหนัก ค่าปริมาณน้ำเกลือที่เหมาะสมที่หาได้คืออัตราส่วนร้อยละ 5 โดยน้ำหนัก ตัวอย่างภายใต้
การอัดตัวคายน้ำเป็นระยะเวลา 2, 7, 15 และ 30 วัน ถูกนำมาทดสอบเพื่อหาค่ากำลังรับแรงในแกน
เดียว ภายใต้ความเค็มกดินในแนวแกน 2.5, 5 และ 7.5 เมกะปาสคาล ค่ากำลังรับแรงในแกนเดียวมีค่า
เพิ่มขึ้นด้วยการเพิ่มขึ้นของระยะเวลาการอัดตัวคายน้ำและมีค่าลดลงเมื่อปริมาณของตะกอนประปา
เพิ่มขึ้น ค่าความซึมผ่านมีค่าลดลงเมื่อปริมาณตะกอนประปาเพิ่มขึ้น ผลการทดสอบได้ถูกนำมาใช้
ในการพัฒนาชุดของสมการเชิงประจักษ์เพื่อใช้ในการออกแบบตัวแปรเบื้องต้นในรูปของคุณสมบัติ
เชิงกายภาพ คุณสมบัติเชิงกลศาสตร์และคุณสมบัติเชิงชลศาสตร์ของส่วนผสมดินตะกอนประปากับ
เกลือบด การจำลองทางคอมพิวเตอร์ได้ถูกดำเนินการเพื่อแสดงประสิทธิภาพของวัสดุถมกลับใน
เหมืองเกลือ อัตราส่วนของตะกอนประปาผสมกับเกลือเกลือ 25:75 โดยน้ำหนัก ค่อนข้างเหมาะสม
มากที่สุดสำหรับใช้เป็นวัสดุถมกลับเพราะมีค่าคุณสมบัติเชิงกลศาสตร์สูงและค่าความซึมผ่านต่ำ

สาขาวิชา เทคโนโลยีธรณี
ปีการศึกษา 2558

ลายมือชื่อนักศึกษา _____
ลายมือชื่ออาจารย์ที่ปรึกษา _____

ADISON BUMRUNGSUK : LABORATORY DETERMINATION OF
MECHANICAL AND HYDRAULIC PROPERTIES OF CONSOLIDATED
SLUDGE-CRUSHED SALT MIXTURES FOR BACKFILLING IN SALT
AND POTASH MINES : THESIS ADVISOR : PRACHYA TEPNARONG,
Ph.D., 114 PP.

STRENGTH/PERMEABILITY/SURFACE SUBSIDENCE/BACKFILL

The objective of this study is to determine the strength and permeability of sludge-crushed salt mixtures as affected by stresses and consolidation period. The sludge-to-crushed salt ratios vary from 0:100, 25:75, 50:50, 75:25 to 100:0 by weight. The optimum brine content is determined as 5% by weight. The samples after consolidation for 2, 7, 15 and 30 days are tested to determine the uniaxial compressive strength under applied axial stress of 2.5, 5 and 7.5 MPa. The uniaxial compressive strengths increase with increasing consolidation time and decrease with increasing sludge content. The permeability decreases as the sludge content increases. The test results are used to develop a set of empirical equations for the design of initial installation parameters in terms of the physical, mechanical and hydraulic properties of sludge-crushed salt mixtures. Computer simulations as performed to demonstrate the effectiveness of backfill materials in salt mine. The mixture ratio of 25:75 by weight is probably the most suitable for backfill material because their high mechanical properties and low permeability.

School of Geotechnology

Academic Year 2015

Student's Signature_____

Advisor's Signature_____

ACKNOWLEDGMENTS

I wish to acknowledge the funding supported by Suranaree University of Technology (SUT).

I would like to express my sincere thanks to Dr. Prachya Tepnarong for his valuable guidance and efficient supervision. I appreciate his strong support, encouragement, suggestions and comments during the research period. My heartiness thanks to Prof. Dr. Kittitep Fuenkajorn and Asst. Prof. Dr. Decho Phueakphum for their constructive advice, valuable suggestions and comments on my research works as thesis committee members. Grateful thanks are given to all staffs of Geomechanics Research Unit, Institute of Engineering who supported my work.

Finally, I would like to thank beloved parents for their love, support and encouragement.

Adison Bumrungsuk

TABLE OF CONTENTS

	Page
ABSTRACT (THAI)	I
ABSTRACT (ENGLISH).....	II
ACKNOWLEDGEMENTS.....	III
TABLE OF CONTENTS.....	IV
LIST OF TABLES.....	VII
LIST OF FIGURES	VIII
SYMBOLS AND ABBREVIATIONS.....	XII
CHAPTER	
I INTRODUCTION	1
1.1 Background and rationale	1
1.2 Research objectives.....	2
1.3 Research methodology.....	2
1.3.1 Literature review.....	2
1.3.2 Sludge-crushed salt mixtures preparation.....	4
1.3.3 Fabrication of test cylinder	4
1.3.4 Laboratory testing.....	5
1.3.5 Derivation of empirical equations	5
1.3.6 Computer simulations.....	6

TABLE OF CONTENTS (Continued)

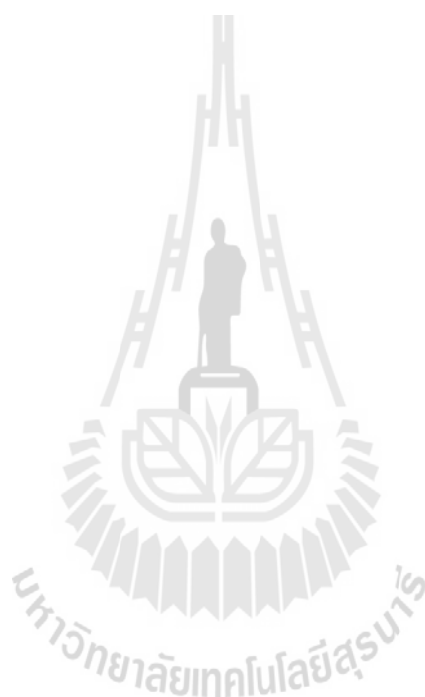
	Page
1.3.7 Discussion, conclusions and thesis writing	6
1.4 Scope and limitations of the study	6
1.5 Thesis contents	7
II LITERATURE REVIEW	8
2.1 Literature review	8
2.2 Consolidation test	13
2.3 Compaction test	24
2.4 Numerical model	31
2.5 Rock salt in northeast region of Thailand	35
III SAMPLE PREPARATION	37
3.1 Introduction	37
3.2 Sludge-crushed salt mixture preparations	37
3.3 Fabrication of test cylinder	41
IV LABORATORY TESTING	42
4.1 Introduction	42
4.2 Suitable brine content of Sludge	42
4.3 Consolidation test and results	42
4.4 Nitrogen flow test and results	44
4.5 Uniaxial compressive strength test and results	47
V DEVELOPMENT OF EMPIRICAL EQUATIONS	58
5.1 Introduction	58

TABLE OF CONTENTS (Continued)

	Page
5.2 Uniaxial strain condition.....	58
5.3 Empirical equations	62
5.3.1 Mean stress of sludge-crushed salt mixtures	62
5.3.2 Volumetric strain of sludge-crushed salt mixture.....	65
5.3.3 Permeability of sludge-crushed salt mixture	68
5.3.4 Density of sludge-crushed salt mixture	70
5.3.5 Uniaxial compressive strength of sludge-crushed salt mixture.....	73
5.3.6 Elastic modulus of sludge-crushed salt mixture	76
5.3.7 Poisson's ratio of sludge-crushed salt mixture	79
VI COMPUTER SIMULATIONS	82
6.1 Introduction.....	82
6.2 Numerical simulations	82
6.3 Results.....	85
6.3.1 Overburden thicknesses	85
6.3.2 Opening height.....	86
6.3.3 Duration before backfill.....	87
VII DISCUSSIONS, CONCLUSIONS AND RECOMMENDATION FOR FUTURES STUDIES.....	100
7.1 Discussions	100
7.2 Conclusions.....	103
7.3 Potential applications	104

TABLE OF CONTENTS (Continued)

	Page
7.4 Recommendations for futures studies.....	105
REFERENCE	107
BIOGRAPHY	114



LIST OF TABLES

Table	Page
5.1	Parameters of mean stresses relationship63
5.2	Parameters of volumetric strain relationship66
5.3	Parameters of intrinsic permeability relationship.....68
5.4	Parameters of density relationship.....71
5.5	Parameters of uniaxial compressive strength relationship..74
5.6	Parameters of elastic modulus relationship..77
5.7	Parameters of Poisson's ratio modulus relationship.....80
6.1	Creep properties of rock salt used in FLAC simulations...84
6.2	Parameters of rock used in FLAC simulations.....84
6.3	Material properties used in FLAC simulations...85
6.4	Results of subsidence in FLAC simulations.....97
6.5	Results of roof in FLAC simulations.....97
6.6	Results of floor in FLAC simulations....98
6.7	Results of pillar width in FLAC simulations.....98
6.8	Results of pillar height in FLAC simulations.....99
7.1	Comparison the properties between sludge and bentonite.....102
7.2	Comparison of mechanical and hydraulic properties between sludge-crushed salt mixtures 25:75 by weight and bentonite-crushed salt mixtures 30:70 by weight.....106

LIST OF FIGURES

Figure	Page
1.1 Research methodology.....	3
2.1 The volumetric strains vs. time data from triaxial consolidation of moderately digested sludge.....	9
2.2 Permeability of intact and crushed salt as a function of porosity.....	14
2.3 Reduction in porosity of crushed salt due to creep consolidation at various seal location-permain basin repository	15
2.4 Measured and predicted permeability versus dry fractional density for the compacted crushed salt column.....	20
2.5 Numerical predicted and test measured mean strain	22
2.6 Typical result of the impact of flocculant on the large consolidation parameters.	23
2.7 Compaction as a function of water content and particle size gradation.	25
2.8 Shear consolidations at a mean stress of 2.33 MPa.....	27
2.9 Shear consolidations at a mean stress of 3.33 MPa.....	27
2.10 Volumetric strain and brine flow as function of time.	28
3.1 Sludge dried in a hot-air oven at 100°C.	38
3.2 Sludge.....	38
3.3 Salt sample crushed by hammer mill..	39
3.4 Crushed salt	40

LIST OF FIGURES (Continued)

Figure	Page
3.5 Grain size distribution of sludge and crushed salt.....	40
3.6 Cylindrical steel tubes.	41
4.1 Axial strain (ϵ_{ax}) as a function of time (t) for different brine contents.....	43
4.2 Test arrangement for consolidation and permeability testing.	43
4.3 Axial strain (ϵ_{ax}) as a function of time (t) for different axial stresses (σ_{ax}).....	45
4.4 Nitrogen gas flow test.....	46
4.5 Intrinsic permeability (k) as a function of time (t) and for different axial stresses (σ_{ax}).	47
4.6 Sludge-crushed salt mixture specimens after consolidation.....	48
4.7 Density (ρ) as a function of consolidation time (t) for different consolidation stresses (σ_{ax})..	49
4.8 Arrangement of uniaxial compressive strength testing	50
4.9 Some post-tested sludge-crushed salt mixture specimens after uniaxial compressive strength testing.	50
4.10 Uniaxial stress-strain curves of specimens after 2 days of consolidation	51
4.11 Uniaxial stress-strain curves of specimens after 7 days of consolidation.	52
4.12 Uniaxial stress-strain curves of specimens after 15 days of consolidation	53
4.13 Uniaxial stress-strain curves of specimens after 30 days of consolidation	54
4.14 Uniaxial compressive strengths (σ_c) as a function of consolidation time (t) for different consolidation stresses (σ_{ax}).	55

LIST OF FIGURES (Continued)

Figure	Page
4.15 Elastic modulus (E) as a function of consolidation time (t) for different consolidation stresses (σ_{ax}).....	56
4.16 Poisson's ratio (ν) as a function of consolidation time (t) for different consolidation stresses (σ_{ax}).....	57
5.1 Lateral stresses (σ_3) as a function of time (t) for different axial stresses (σ_{ax})	60
5.2 Mean stresses (σ_m) as a function of time (t) for different axial stresses (σ_{ax}).	61
5.3 Mean stresses (σ_m) as a function of time (t) and axial stresses (σ_{ax}), test result (point) and back prediction (lines).....	64
5.4 Volumetric strain ($\Delta v/v$) as a function of time (t) and mean stresses (σ_m), test result (points) and back prediction (lines)..	67
5.5 Intrinsic permeability (k) as a function of time (t) and mean stresses (σ_m), test result (points) and back prediction (lines)	69
5.6 Density (ρ) as a function of time (t) and mean stresses (σ_m), test result (points) and back prediction (lines).....	72
5.7 Uniaxial compressive strength (σ_c) as a function of time (t) and mean stresses (σ_m), test result (points) and back prediction (lines).....	75
5.8 Elastic modulus (E) as a function of time (t) and mean stresses (σ_m), test result (points) and back prediction (lines).	78

LIST OF FIGURES (Continued)

Figure	Page
5.9	Poisson's ratio (ν) as a function of time (t) and mean stresses (σ_m), test result (points) and back prediction (lines)81
6.1	Simplified stratigraphy column of rock salt and clastic rock at Ban Khao, Muang district Udon Thani province.....83
6.2	Finite difference mesh constructed to simulate formation of overburden thickness varied from 100, 150 to 200 m and rock salt is 30 m.....88
6.3	Finite difference mesh constructed to simulate formation of overburden thickness 100 m, rock salt is 30 m and opening height varied from 2, 4 and 6 m (borehole no. K-089).89
6.4	Surface subsidence as a function of time (t) for different sludge contents where overburden thicknesses = 100 m, duration before backfill = 24 month and opening height = 4 m90
6.5	Surface subsidence as a function of time (t) for different sludge contents where overburden thicknesses = 150 m, duration before backfill = 24 month and opening height = 4 m91
6.6	Surface subsidence as a function of time (t) for different sludge contents where overburden thicknesses = 200 m, duration before backfill = 24 month and opening height = 4 m.92

LIST OF FIGURES (Continued)

Figure	Page
6.7 Surface subsidence as a function of time (t) for different sludge contents where overburden thicknesses = 100 m, duration before backfill = 24 month and opening height = 2 m	93
6.8 Surface subsidence as a function of time (t) for different sludge contents where overburden thicknesses = 100 m, duration before backfill = 24 month and opening height = 6 m	94
6.9 Surface subsidence as a function of time (t) for different sludge contents where overburden thicknesses = 100 m, duration before backfill = 6 month and opening height = 4 m	95
6.10 Surface subsidence as a function of time (t) for different sludge contents where overburden thicknesses = 100 m, duration before backfill = 12 month and opening height = 4 m	96

SYMBOLS AND ABBREVIATIONS

ρ	=	Density
μ	=	Dynamic viscosity
α	=	Empirical constant
β	=	Empirical constant
δ	=	Empirical constant
ϕ	=	Empirical constant
γ	=	Empirical constant
η	=	Empirical constant
φ	=	Empirical constant
κ	=	Empirical constant
Ω	=	Empirical constant
ζ	=	Empirical constant
ι	=	Empirical constant
λ	=	Empirical constant
μ	=	Empirical constant
υ	=	Empirical constant
ε	=	Empirical constant
ς	=	Empirical constant

SYMBOLS AND ABBREVIATIONS (Continued)

ω	=	Empirical constant
ω	=	Empirical constant
ξ	=	Empirical constant
$\hat{\sigma}$	=	Empirical constant
ν	=	Poisson's ratio
ρ_0	=	Initial density
$\varepsilon_2, \varepsilon_3$	=	Lateral strain
σ_2, σ_3	=	Lateral stress
$\varepsilon_{ax}, \varepsilon_1$	=	Axial strain
σ_{ax}, σ_1	=	Axial stress, Consolidation stress
σ_C	=	Uniaxial compressive strengths
γ_f	=	Unit weight of fluid
Δh	=	Head different
ΔL	=	Length changes over time
σ_m	=	Mean stress
ΔP	=	Pressure different
$\Delta v/v$	=	Volumetric strain
e	=	Void ratio
k	=	Intrinsic permeability
K	=	Permeability coefficient

SYMBOLS AND ABBREVIATIONS (Continued)

L	=	Length
m	=	Weight
N ₂	=	Nitrogen gas
Q	=	Flow rate
t	=	Time of consolidation
v	=	Volume



CHAPTER I

INTRODUCTION

1.1 Background of problems and significance of the study

Surface subsidence due to the deformation of pillar and roof of underground openings is a problem for salt and potash mining. This problem may impact surface structure, farmland, reservoir and groundwater. One of the remediation is to return the waste crushed salt to the mine out openings to reduce the roof and pillar deformation. Crushed salt has been widely recognized as the most suitable backfill material (Case and Kelsall, 1987). The primary advantages of crushed salt are the availability, low cost and obvious compatibility with host rock (Stormont and Finley, 1996). Somtong et al. (2013) have found that the volumetric strain and density of crushed salt increase with consolidation time and applied stresses. The porosity and permeability decrease with increasing density (Case and Kelsall, 1987; Loken and Statham, 1997; Hansen and Mellegard, 2002). Brodsky et al., (1995) conduct hydrostatic and triaxial compression tests with brine content of 2.5% to 3% by weight. The results indicate that the permeability decreases approximately 2.1 orders of magnitude as fractional density increases from 0.9 to 1. The unconfined compressive strength and Young's modulus of crushed rock salt also increase with respect to densification time (Miao et al., 1995) and decreases with porosity (Kelsall et al., 1984). However, using only crushed salt may lead to highly time-dependent deformation of the openings to be backfilled because the crushed salt consolidates significant by under applied load.

A common solution practiced internationally in the mining industry is to use bentonite-crushed salt as a backfill material to reduce permeability and deformation in salt mine opening. However, bentonite is expensive and exhibits low strength. Wetchasat and Fuenkajorn (2013) suggest that sludge can be used as a substitute material for bentonite to be mixed with cement and water to grout rock fractures.

1.2 Research objectives

The objective of this study is to determine the mechanical and hydraulic properties of sludge-to-crushed salt mixtures by consolidation tests. The task involves performing consolidation tests on various ratios of the sludge-to-crushed salt, and uniaxial compression strength test and gas flow tests to determine the mechanical and hydraulic properties of the mixtures. The test results will be used to develop a set of empirical equations to design the initial installation parameters in terms of the physical, mechanical and hydraulic properties of the sludge-crushed salt backfill as a function of time.

1.3 Research methodology

The research methodology shown in Figure 1.1 comprises 7 steps; including literature review, sample preparation, fabrication of test cylinder, consolidation permeability and uniaxial compressive strength tests, development of empirical equations, computer simulations and discussions and conclusions.

1.3.1 Literature Review

Literature review will be carried out to study the previous researches on consolidation testing, mechanical and hydraulic properties and computer simulations of

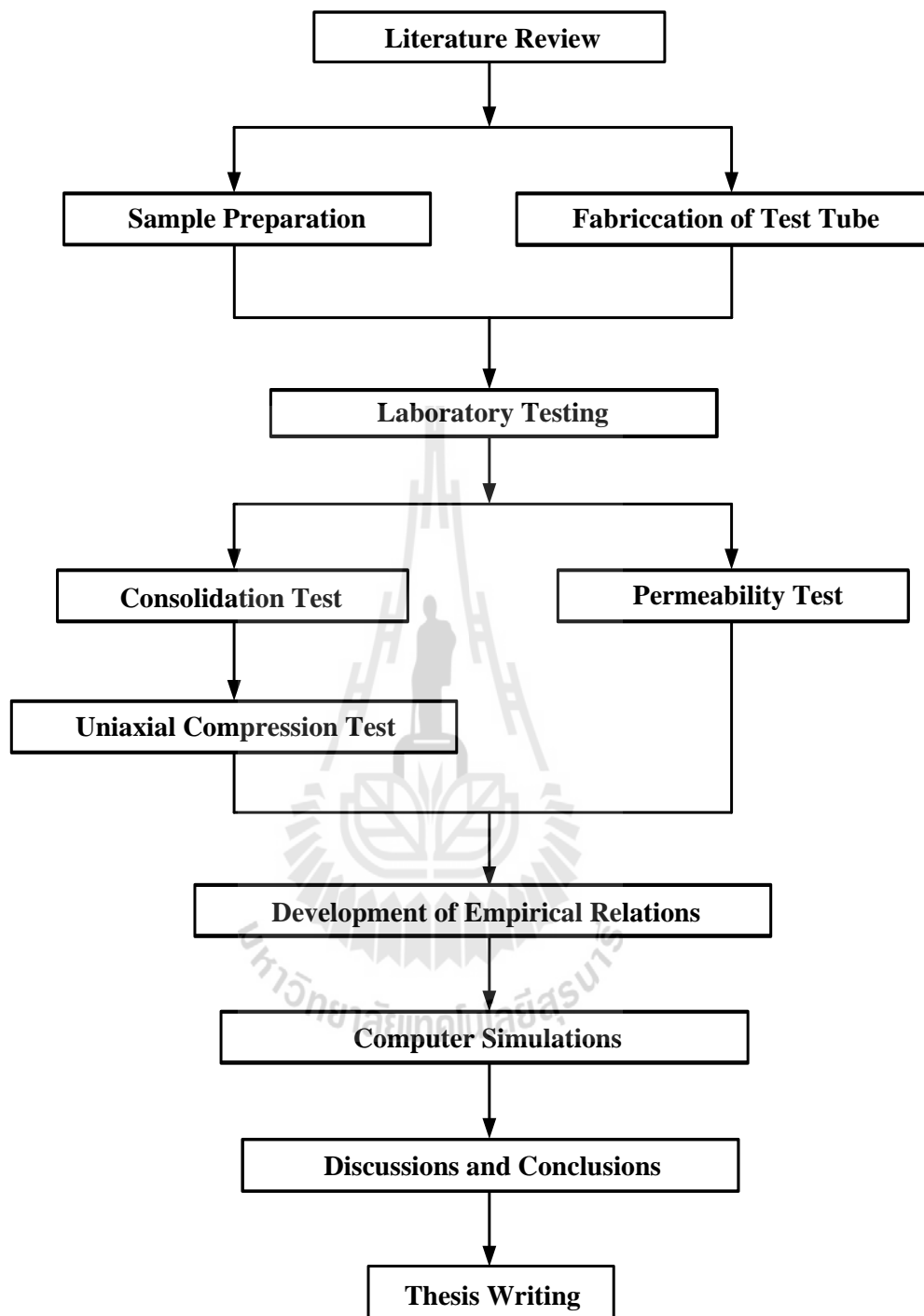


Figure 1.1 Research methodology

ballast material-crushed salt mixtures. The sources of information are from text books, journals, technical reports and conference papers. A summary of the literature review will be given in the thesis.

1.3.2 Sludge-Crushed Salt Mixtures Preparation

Sludge used in this study is prepared from the Metropolitan Waterworks Authority in Bangkok. It is dried under sunlight. The moisture is removed again in a hot-air oven at 100°C for at least 24 hours or until its weight remains constant. The dried sludge is sieved through a mesh no. 40 to obtain grain sizes ranging from 0.001 to 0.475 mm. Crushed salt used in this study have been obtained from the Middle member of the Maha Sarakham formation in the Korat basin, northeastern Thailand. The grain sizes of crushed salt range from 0.075 to 2.35 mm. The ratios of sludge-crushed salt mixtures vary from 0:100, 25:75, 50:50, 75:25 to 100:0 by weight. The 5% by weight of saturated brine is added to the sludge-crushed salt mixtures. The optimum brine content are performed by applying axial stresses on loading steel piston to the sludge mixed with 2.5, 5, 7.5 and 10% of saturated brine. The axial stress is 2 MPa. All tests are conducted under ambient temperature for 96 hours at the 2.5, 5, 7.5 and 10% of brine contents. The density of the consolidation specimens is similar. The proportion of saturated brine to crushed salt in this study is therefore determined as 5% by weight.

1.3.3 Fabrication of Test Cylinder

The cylindrical steel tube with 54 mm internal diameter, 64 mm outside diameter and 200 mm height is used as consolidation tube. Two load platens having 53 mm diameter with 100 mm length are to applied axial load to the crushed salt specimens. Two o-rings are installed around each load platen. There is a 10 mm

diameter hole at the center of the top and bottom load platens for use as inlet of N₂ to specimens for permeability testing and drained water from specimen.

1.3.4 Laboratory Testing

The consolidation tests are performed by applying constant axial stresses from a hydraulic load pump to the sludge-crushed salt mixtures samples installed in the 54 mm diameter steel cylinders. The constant axial stresses are 2.5, 5 and 7.5 MPa. All tests are conducted under ambient temperature. The axial displacements are continuously measured as a function of time by dial gages to calculate the changes of axial strain, density, and void ratio. The nitrogen gas flow testing is performed to determine intrinsic permeability of crushed salt consolidation that changes over time. The flow rates under constant head are continuously monitored every 6 hours. The compressive strength of the consolidated crushed salts samples is determined by axially loading the crushed salt cylinder (after removing from the steel tube) with a nominal diameter of 54 mm and L/D ranging from 2 to 3. Uniaxial compressive strength measurements are made after 2, 7, 15 and 30 days of consolidation.

1.3.5 Derivation of Empirical Equations

The physical, hydraulic and mechanical results are used to develop a set of empirical equations by SPSS statistical software to design the initial installation parameters in terms of the physical, mechanical and hydraulic properties of the sludge-crushed salt mixtures. The equations will correlate between the applied stresses and consolidation time with volumetric strain, void ratios, densities, permeability, uniaxial compressive strengths and elastic parameter of the consolidated sludge-crushed salt mixtures.

1.3.6 Computer Simulations

The computer simulation is to determine the effectiveness of backfill in salt and potash mines after the excavation completed. The finite difference analyses are performed using FLAC 4.0 (Itasca, 1992) to assess the time-dependent surface subsidence and the deformation of rooms and pillars.

1.3.7 Discussions, Conclusions and Thesis Writing

All research activities, methods, and results will be documented and compiled in the thesis. The research or findings will be published in the conference proceedings or journals.

1.4 Scope and limitations of the study

The scope and limitation of the research include as follows.

1. Crushed salt sample will be obtained from the Maha Sarakham formation. The crushed salt has grain sizes ranging from 0.075 to 2.36 mm.
2. The dried sludge will be sieved through mesh no. 40 to obtain grain sizes ranging from 0.001 to 0.475 mm.
3. Consolidation tests will be performed by applying constant axial stresses on loading steel piston to the mixtures installed in the 54 mm diameter steel cylinder with length 200 mm.
4. Suitable brine content will be determined.
5. Ratios of sludge-crushed salt mixtures vary from 0:100, 25:75, 50:50, 75:25 to 100:0 by weight.
6. Sludge-crushed salt mixtures are consolidated for 2, 7, 15 and 30 days with

applied constant axial stresses of 2.5, 5 and 7.5 MPa.

7. Nitrogen gas flow tests will be performed on sludge-crushed salt mixtures during consolidation.
8. Uniaxial compression tests will be performed on the specimens after removing from test tube.
9. All tests will be conducted under ambient temperature.
10. The research findings will be published in conference paper or journal.

1.5 Thesis contents

The first chapter introduces the thesis by briefly describing the background of problems and significance of the study. The research objectives, methodology, scope and limitations are identified. Chapter second summarizes the results of the literature review. Chapter three describes the sludge-crushed salt preparation and the fabrication of test cylinder. The laboratory tests and results of all tested are presented in chapter four. Laboratory test are divided into 3 tests, including 1) Consolidation tests 2) Permeability tests 3) Uniaxial compressive tests. The development of empirical equation are describes in chapter five. Chapter six present computer simulation. Chapter seven provide the discussions, conclusions, potential applications and recommendation for futures studies.

CHAPTER II

LITERATURE REVIEW

2.1 Literature Review

Relevant topics and previous research results are reviewed to improve an understanding of the physical, hydraulic and mechanical properties of sludge-crushed salt mixtures are affected by stress and consolidation time. The results of the literature review are presented below, including experimental researches on the basic properties of sludge, compaction test and consolidation test.

2.2 Basic Properties of Sludge

Laothong (2003) studies the sludge cake from the water treatment process at Wang Noi Power Plant. The results indicate that the sludge is a nonhazardous waste. There are 300 tons of the sludge per month, costing 2.48 baht/kg or 460,000 baht per month for disposal. The utilization of the sludge cake can reduce operation cost of the power plant. The sludge is found to be loamy sand. Four sludge cake utilization alternatives have been explored, including cement replacement in mortar, laterite replacement in interlocking block, clay replacement in baked clay brick and ceramic wares. The results indicate that the best alternative is laterite replacement in interlocking block with the proportion of 2:2:5 by weight (cement:sludge:laterite). With the interlocking block alternative, although the production cost of 3.83 baht/kg was higher than disposal cost of 1.35 baht/kg, the product could be sold at the price of

about 6 to 8 baht. Utilization of sludge cake in making interlocking block is being considered to be a feasible alternative.

O'Kelly (2004) study mechanical properties of dewatered, anaerobically digested sewage sludge. The sludge material is largely composed of organic clay size-particles. The specific gravity of sludge had 1.55. The maximum dry density of 0.56 tonne/m³ for the dried sludge material was produced using standard proctor compaction at roughly 85% moisture content (54% solids content). The ϕ value increase from 32° for moderately digested sludge, to 37° for strong digested sludge. The effective cohesion of the sludge material remained zero throughout. The sets of sample were then consolidation until effective confining pressure of 30, 60 and 140 kPa. The volumetric strains increase with consolidation time show in Figure 2.1.

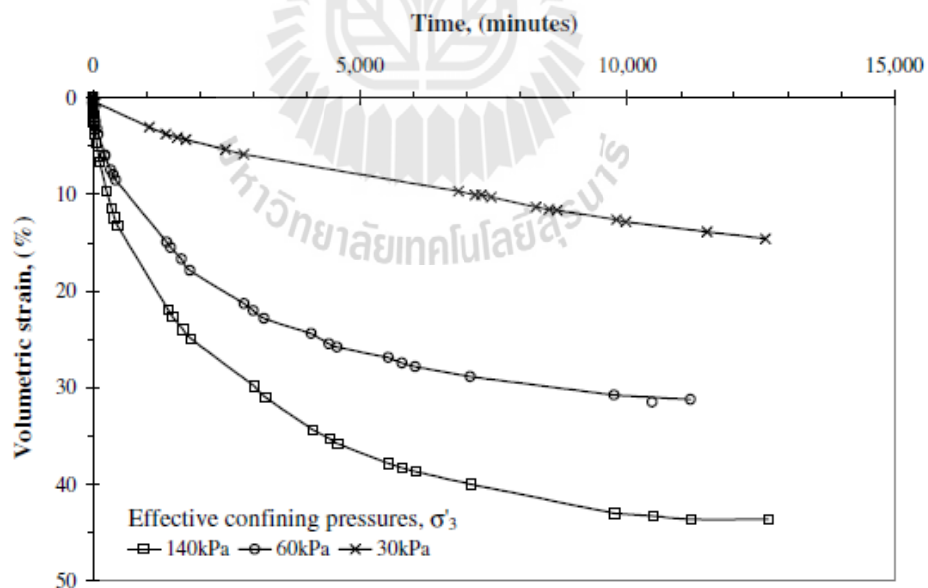


Figure 2.1 The volumetric strains vs. time data from triaxial consolidation of moderately digested sludge. (O'Kelly, 2004)

Suriyachat et al. (2004) study the basic properties of the water treatment sludge. The results indicate that the liquid limit is 77.96%, plastic limit is 50.76%, shrinkage limit is 11.15%, the plasticity index is 27.20%, and the maximum density is 1.33 g/cm³. The correlation between permeability coefficient and the moisture content is found when the moisture content is low with high permeability coefficient. This is probably a result of a rearrangement of molecules at the particle surfaces by the action of adsorbing water leading to a formation of gain-soil bridges. The optimum moisture content of 29% is suitable for the minimum coefficient of permeability. The coefficient of permeability is similarly to the clay used in the ceramic industry.

The chemical compositions of the sludge and clay from the pottery in central and northern parts of Thailand suggest that the sludge properties are similar to the clay properties of these manufacturers. The analysis of chemical compositions shows that the amount of Fe₂O₃ is between 4 and 5%, including the optimal values of SiO₂ and Al₂O₃ as it is similar to red clay. This is an important raw material used in the ceramic industry.

Laboratory experiments in ceramic product made of the sludge are in the areas of pottery and jewelry. Those must be mixed with sand. To obtain a beautiful shape it must have the sand portion of 30%, but it takes several times for fermentation of the clay. The initially result showed that the water treatment sludge could be used as a raw material in the ceramic industry. It makes to achieve a renewable and reused in the manufacturing of integrated and sustainable natural materials.

Valls et al. (2004) study sludge additional to concrete with Portland cement. Sludge content of 10 % or more cannot use because significantly delays the setting of

the cement and reduce its mechanical properties, especially in the short term. The compressive strength was 4.5 MPa. After 28 days, the same concrete had reached strength of 6 MPa. And after 90 days, it reached 18 MPa. Deformability of the concrete increases with increasing sludge content. Density of the concrete decrease with an increasing sludge content and increases as the curing time increases. Porosity and absorption coefficient increase with increasing sludge content and decrease as the curing time increase.

Bunjongsiri and Bunjongsiri (2005) study the content of clay mix with sludge from community wastewater treatment to make brick. There are six ratios of clay and sludge from community wastewater treatment: 3:1, 7:3, 6.5:3.5, 3:2, 5.5:4.5 and 3:7. The experiment indicated the quantity of the heavy metal in the brick (mg/kg) and two ratios of 1:3 and 3:7 by leachate extraction procedure. The quantities in mg/kg of the heavy metal were 240.84 and 490.07 for copper, 17.66 and 59.16 for lead, 0.636 and 0.96 for cadmium, 667.87 and 973.28 for manganese, 167.44 and 157.45 for chromium and 136.82 and 337.75 for zinc. The bricks could not reach the industrial standard of TIS 77-2531. The ratio of 3:1 represents the best value close to the industrial standard as the value of compressive strength was 15.05 kg/cm². The density was 1.10 g/cm³. Tolerance of length, wide, and thickness was 5.24, 6.16, and 9.35% respectively. The weight was 388.60 g and the absorber was 36.23%.

Poonsawat and Lertpocasombut (2006) study the properties of tile bodies to produce clay plan roofing tile by using sludge from Bang Khen and Mahasawat water treatment plants as a raw material. The tile bodies are consisted of 70 to 100% of the sludge and 0 to 30% of quartz and feldspar. They are fired at 1,000, 1,050 and 1,100°C. The results indicate that the plasticity index of the sludge from Bang Khen

water treatment plant is higher than those from Mahasawat water treatment plant. Temperature increases the strength, shrinkage and bulk density and decreases water absorption and porosity. At 1,100°C, the ratios of 90:5:5 (Bang Khen sludge:quartz:feldspar) and 85:5:10 (Mahasawat sludge:quartz:feldspar) are suitable for making clay plan roofing tile.

Kongthong and Lertpocasombut (2006) study adsorption by using sludge from Bang Khen water treatment plant. Research objective was aimed to reduce color remaining of effluent wastewater from dye industries. Fifty mg/l of three solutions (basic, reactive, and disperse dyes) is used as initial concentration. Sludge ash which is obtained after burning at 500°C and dried sludge is used as an adsorbent. The pH results showed no effect on the adsorption of the basic and re-active dyes while disperse to dye is effectively adsorbed at pH 4. Equilibrium time and isotherm of the adsorption are determined and found that the dried sludge gave good results compared to the sludge ash in basic dye adsorption. It is in contrast to the disperse dye adsorption. The results are not found in re-active dye adsorption either using dried sludge or sludge ash.

Sangiumsak and Cheerarot (2008) determine the properties of artificial aggregates made from the water treatment sludge. The aggregates containing various proportions between the sludge and clay, 100:0, 80:20, 60:40, 40:60, 20:80 and 0:100 by weight were prepared by molding and firing at 800, 1,000, and 1,200°C for 24-hour firing time. Then compressive strength of an artificial aggregate is tested. Some mixtures are chosen to test abrasion, stability in sodium sulfate, and absorption. Finally, the compressive strength of concrete containing the artificial aggregates is tested. The results showed that the compressive strength of the artificial aggregates

increased with increasing firing temperature and amount of sludge. The aggregates with the ratio of sludge to clay of 60:40 fired at 1,200°C had the highest compressive strength of 490 ksc. The aggregate fired at 1,200°C had the highest compressive strength while the aggregate fired at 800 and 1,000°C gave similar compressive strengths. When the amount of the sludge increased, the water absorption, abrasion, and stability in sodium sulfate of the aggregates decreased. Comparing with natural aggregates, the water absorption of all proportions of the artificial aggregates was higher than that of the natural aggregates. The abrasion and stability in sodium sulfate were low. The concrete containing the artificial aggregates had higher compressive strength than the concrete containing natural aggregates.

Wetchasat and Fuenkajorn (2013) study the performance of sludge mixed with the commercial grade Portland cement type I for use in reducing permeability of fractures in sandstone. The results of laboratory studies aim at determining appropriate grout mixes proportion from sludge-mixed cement for reducing permeability in saturated fractured rock under various stresses in the laboratory and to compare the results with the bentonite-mixed cement in terms of the mechanical and hydraulic properties. Three mixtures of S:C are 1:10, 3:10 and 5:10 that are closely similar in terms of the mechanical and hydraulic properties. Those are some important differences in their viscosity. The minimum and maximum viscosities of S:C are 1:10 and 5:10 by weight.

2.2 Consolidation Test

Shor et al. (1981) study consolidated crushed salt in brine and obtained a relationship between permeability, porosity and average initial particle size. The

initial particle size in this study various mixes range from 0.01 to 0.03 cm. The relationship between permeability and porosity is shown in Figure 2.2. The result indicated that the permeability of crushed salt is lower than those intact rock salt data.

Kelsall et al. (1984) present the properties of crushed salt and the nature of fracture healing as known from laboratory testing and presents analytical methods for predicting the rates at which the processes will occur in a repository. The range of grain size for the crushed material is 75 mm to about 0.05 mm. The result indicate that consolidations to low porosities should occur within hundreds of years at most candidate repository sites for locations within the repository close to the waste (Figure 2.3). Fracture healing should occur relatively rapidly, within tens to hundreds of

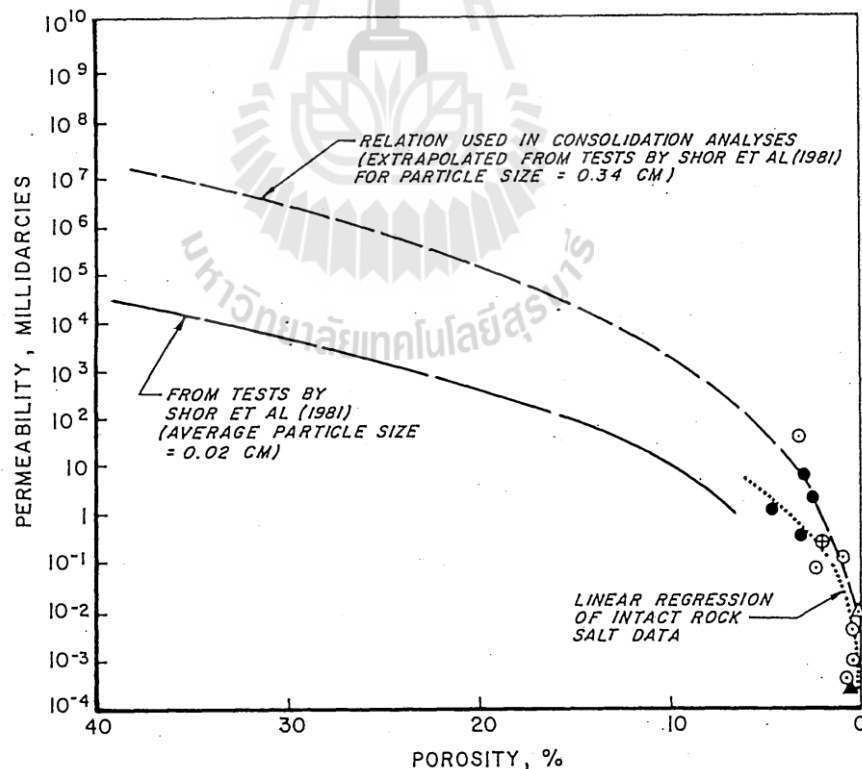


Figure 2.2 Permeability of intact and crushed salt as a function of porosity (Shor et al., 1981).

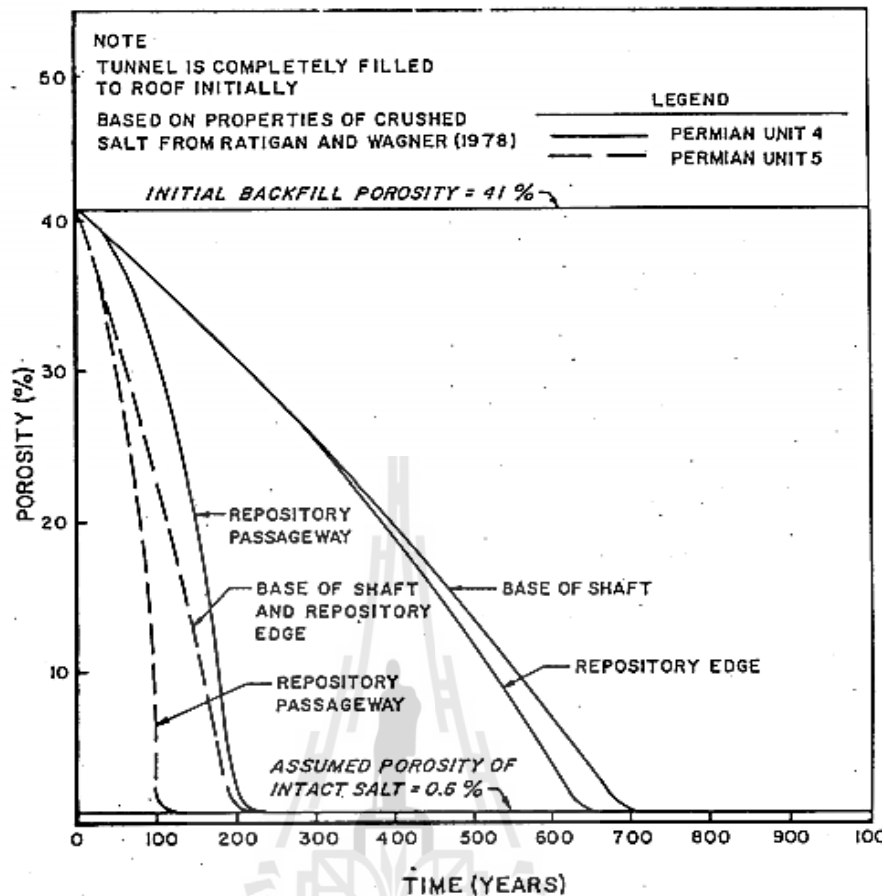


Figure 2.3 Reduction in porosity of crushed salt due to creep consolidation at various seal location-permain basin repository (Kelsall et al., 1984).

years, as the confining stress across the fractures approaches lithostatic levels. Healing of fractures caused by excavation may be enhanced by placing relatively rigid concrete plugs in the tunnel openings.

Case and Kelsall (1987) study the potential of crushed salt for required sealing access shafts and drifts for long periods. Crushed salt backfill is being investigated as a potential backfill and seal material through laboratory testing to determine how fundamental properties such as permeability, porosity and creep rate are reduced by pressure and time through consolidation. The test program consisted of four

consolidation tests using crushed salt obtained from the Waste Isolation Pilot Plant and the Avery Island Mine. Tests with one-month or two-month durations were conducted on samples with maximum particle sizes of 1, 10, and 20 mm, with initial porosities ranging from 26 to 36%, moisture contents of zero and 2%, and initial permeability from 10^3 to 10^5 m². The tests were performed at ambient temperature and confining pressures ranging from 0.34 MPa to 17 MPa. The most significant observation from the tests was the influence of moisture on changes in permeability, porosity and volumetric creep strain rate. The final permeability and porosity of one moist sample were reduced after one month to about 10^{-5} m² and 5%, respectively, compared to about 10^{-2} m² and 14 to 19% for the dry samples. In addition, the consolidation rate for the moist sample was more rapid at comparable porosities. In all of the tests, the volumetric creep strain rate ranged from 10^{-8} to 10^{-6} /sec, and did not achieve steady state values after 1 to 2 months of load application.

Butcher (1991) presents the advantage of a salt-bentonite backfill of Waste Isolation Pilot Plant Disposal Rooms. The salt-bentonite mixture at 70:30 by weight is preferable to pure crushed salt s backfill for disposal rooms. The permeability of salt-bentonite mixture is found to range 10^{-18} to 10^{-19} m². The salt-bentonite mixture is low porosity, chemical stability and sorption potential for brine and radionuclides. The bentonite swelling pressure is between 2.3 to 3.5 MPa.

Pfeifle (1991) study consolidation, permeability and compressive strength tests of bentonite-crushed salt mixtures. Each mixture comprised 30 percent bentonite and 70 percent crushed salt base on total dry weight. The proportion of water content to bentonite-crushed salt mixtures is therefore determined as 5 or 10 percent by weight. The consolidation tests are conducted under hydrostatic stresses between

3.45 and 14 MPa. The volumetric strains increase between 0.2 and 0.3 with increasing hydrostatic stress and consolidation time. Constant rate of flow test show that permeability ranging from $1.3 \times 10^{-17} \text{ m}^2$ to $4.9 \times 10^{-17} \text{ m}^2$. The unconfined compressive strength is ranging from 0.5 to 8.1 MPa. The higher strengths are measured at higher densities.

Brodsky et al. (1995) studies the consolidation and permeability of crushed salt in hydrostatic and triaxial compression. The hydrostatic consolidation test results on nominally saturated specimens from Zeuch et al. (1990) are compared with the Brodsky (1994). The errors in determinations of fractional density are approximately ± 0.02 . The results show that the data from Zeuch et al. (1990) for nominally saturated specimen show less consolidation than do the specimens tested by Brodsky (1994). Some variability in the data is expected because the specimens used by the two laboratories were prepared from different batches of crushed salt. Although grain size analyses were performed and shown to be comparable, small variation in grain size and impurity contents are expected and these can affect the densification mechanisms and the distribution of brine. They have already remarked upon the differences in specimen assemblies that permitted the Sandia specimen to drain less freely than the RE/SPEC specimens.

Triaxial consolidation test results for specimens containing 2.5% to 3.0% brine by weight at small imposes stress differences for test at confining pressures of 3.45 MPa (approximately), 5.17 MPa and 6.90 MPa, respectively. The data indicate that there is no correlation between the magnitudes of small applied axial stress differences and consolidation rates, and the specimen-to specimen variability is large relative to the effect of small stress differences. The results of permeability as a

function of fractional density show that the values of permeability range from 6×10^{-18} m² to 3×10^{-22} m². Permeability decreases approximately 2.1 orders of magnitude as fractional density increase from 0.90 to 1.0.

Daeman and Ran (1996) study the potential of bentonite for required sealing access shaft and drifts for long periods. Bentonite is an engineering material as excellent sealing material. The basic properties of bentonite indicate that liquid limit is 105, Plastic limit is 35, Density 1.8 g/cm³. The composition contains over 90% montmorillonite and small portions of feldspar, biotite, etc. The permeability was less than 10^{-16} m². The compressive strength was ranging from 2.9 to 5.0 MPa. The swell pressure is ranging from 1 to 2 MPa. The optimum brine content was 5% by weight.

Loken and Statham (1997) propose to use crushed salt from the host Salado formation as a sealing material in one component of a multicomponent seal system design for the shafts of the Waste Isolation Pilot Plant (WIPP), a mined geological repository for storage and disposal of transuranic radioactive wastes located near Carlsbad, New Mexico. The crushed salt will be compacted and placed at a density approaching 90 percent of the intact density of the host Salado salt. Creep closure of the shaft will further compact the crushed salt over time, thereby reducing the crushed-salt permeability from the initial state and creating an effective long-term seal. A structural model and a fluid flow model have been developed to provide an estimate of crushed-salt reconsolidation rate as a function of depth, time, and pore pressure. Model results are obtained in terms of crushed-salt permeability as a function of time and depth within the salt column.

The fluid in the crushed salt was assumed to behave as a linear elastic material in which the fluid pressure is related to the volume strain through the bulk modulus as:

$$P = \text{MIN} \{P_0 + K (1 - V/V_0), P_{\max}\} \quad (2.1)$$

where P = fluid pressure (MPa), P_0 = initial fluid pressure (MPa), K = fluid bulk modulus (MPa), V = current volume of crushed salt (m^3), V_0 = initial volume (based on 90 percent fractional density) (m^3) and P_{\max} = maximum fluid pressure (MPa).

A model was developed that relates permeability and density of crushed salt. Laboratory measurements indicate that the permeability decreases as density increases (Figure 2.4). Furthermore, the density of the crushed salt in the column seal will increase with time during reconsolidation because of creep of the surrounding salt. It was determined that a linear model relating permeability (transformed into logarithmic space) and fractional density was a good approximation to the laboratory data over the range of density tested. A linear least-square fit was performed using the following model:

$$\log(k) = m\rho + b \quad (2.2)$$

where k is intrinsic permeability with units of m^2 , ρ is the dimensionless fractional density based on an intact salt density of $2,160 \text{ kg/m}^3$, and m and b are fitting parameters determined to be -54.885 m^2 and 34.613 m^2 , respectively. For a fractional density of one (i.e., density equivalent to intact salt), the model predicts a permeability of $5.34 \times 10^{-21} \text{ m}^2$, which is within an order of magnitude of the assumed

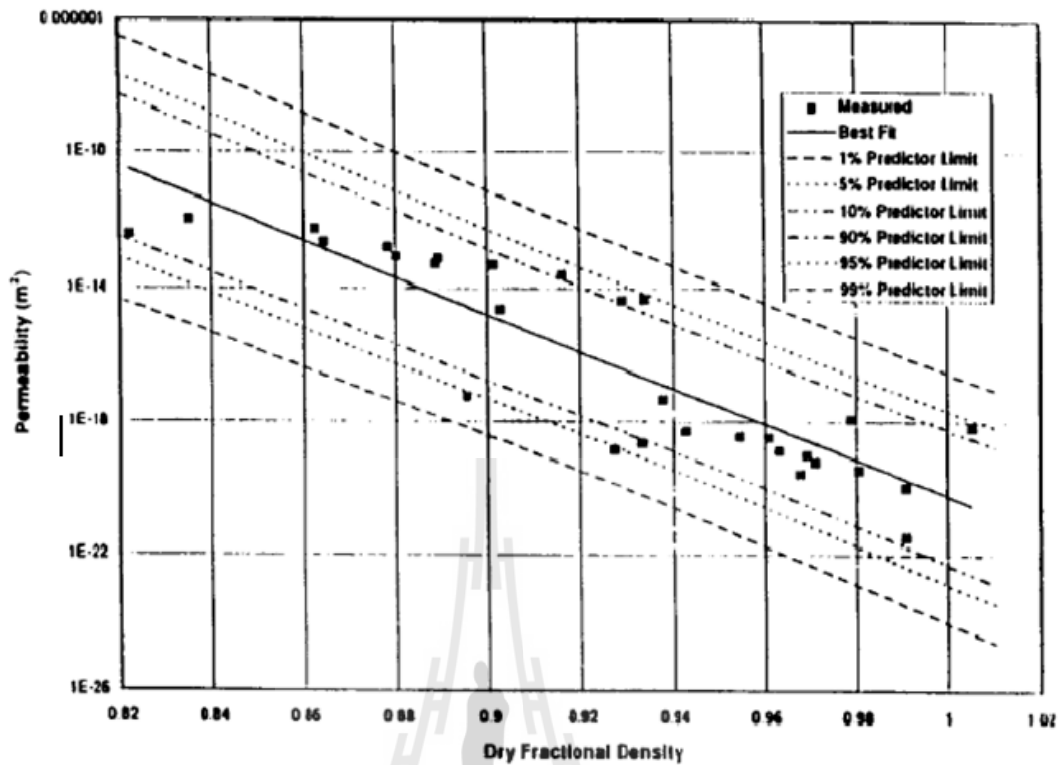


Figure 2.4 Measured and predicted permeability versus dry fractional density for the compacted crushed salt column (Loken and Staham, 1997)

permeability for intact salt; i.e., $1.0 \times 10^{-21} \text{ m}^2$. Model results indicate that average salt column permeability will be reduced to $3.3 \times 10^{-20} \text{ m}^2$ in about 100 year, which provides for an acceptable long-term seal component.

Aydilek et al. (1999) study large-scale and small-scale consolidation test of wastewater treatment sludge were investigated using laboratory and field test. The specimen of small-scale consolidation tests (ASTM D2435) has 50 mm inside diameter and 12 mm height. The large-scale consolidation tests has 50 mm inside diameter and 48 mm height. As a result of the volumetric strains of large-scale test are much higher than small-scale tests because of high initial water contents and void ratio.

Pudewills and Krauss (1999) present the numerical modeling of the thermomechanical behavior of crushed salt using a viscoplastic constitutive model. In the ADINA finite element code the viscoplastic model that considers both volumetric and deviatoric strain rates under hydrostatic and shear stress conditions proposed by Hein (Hein HJ. Ein stoffgesetz zur Beschreibung des thermomechanischen Verhaltens von Salzgranulat. Dissertation, RWTH Aachen, 1991) is implemented. A series of exercises were designed to verify the numerical implementation and the theoretical formulation of the proposed model. The applicability of the model to predicting the consolidation of a crushed salt specimen with step-wise stress increase and decrease, performed in laboratory tests. Mathematical equation proposed by Hein (1991) is as follows:

$$\dot{\epsilon}_{ij} = A \cdot \exp^{-Q/RT} \cdot (h_1 \cdot p^2 + h_1 \cdot q^2)^n \cdot \left(\frac{1}{3} h_1 \cdot p \cdot I + h_2 S_{ij} \right) \quad (2.3)$$

$$h_1 = \frac{a}{[(\eta_0 / \eta)^c - 1] / \eta_0^c + d]^m} \quad (2.4)$$

$$h_2(\eta) = b \cdot h_1(\eta) + 1 \quad (2.5)$$

where $\dot{\epsilon}_{ij}$ is the strain occurring, η is the porosity, η_0 is the initial porosity, T is the absolute temperature, p is the mean stress perpendicular, I was the Tensor metric, Q is the activation energy, R is the gas constant, q is the a variation of stress S_{ij} is the stress deviation tensor, A , b , c , d , m , n are constants of the equation, and the Q / R is a constant equal to 6520 K^{-1} of the consolidation (Odometer test) with strain rate $6.9 \times 10^{-9} \text{ s}^{-1}$. The results are consistent with the results of laboratory tests. The simulation model

and compression stresses increase to 3 levels by 15 days/step, compared to the average stress and the changes of porosity. The results of simulation and experiment were found to be consistent as well. The simulation results will provide a slightly lower value (Figure 2.5).

Van Impe et al. (2009) presents the laboratory setup and some preliminary results of large strain consolidation testing on several types of dredging and industrial waste sludge. The tests are performed investigating the impact of assistive, specifically coagulant and flocculants, on the consolidation behavior of mineral sludge. Figure 2.6 shows the comparison of the compressibility and permeability curve for the original material and the mixtures using a weak flocculant. The compressibility curve it is clear that impact of the flocculant is limited to very low stress levels. The permeability shows an increased value over full range of void ratios.

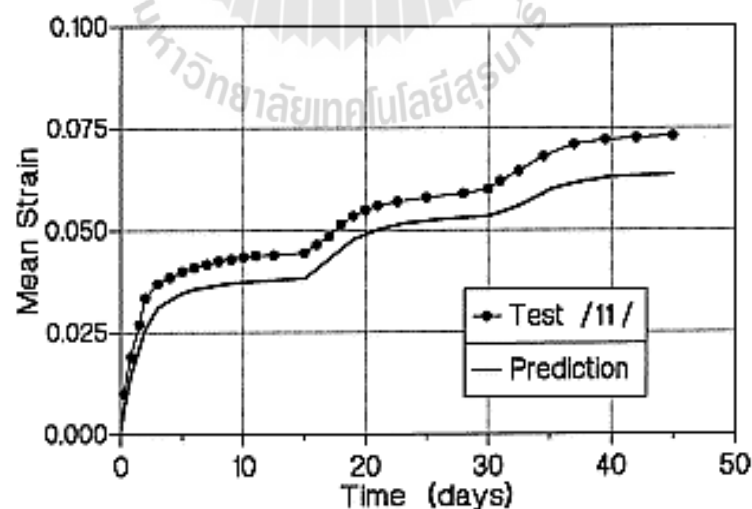


Figure 2.5 Numerical predicted and test measured mean strain (Pudewills and Krauss, 1999).

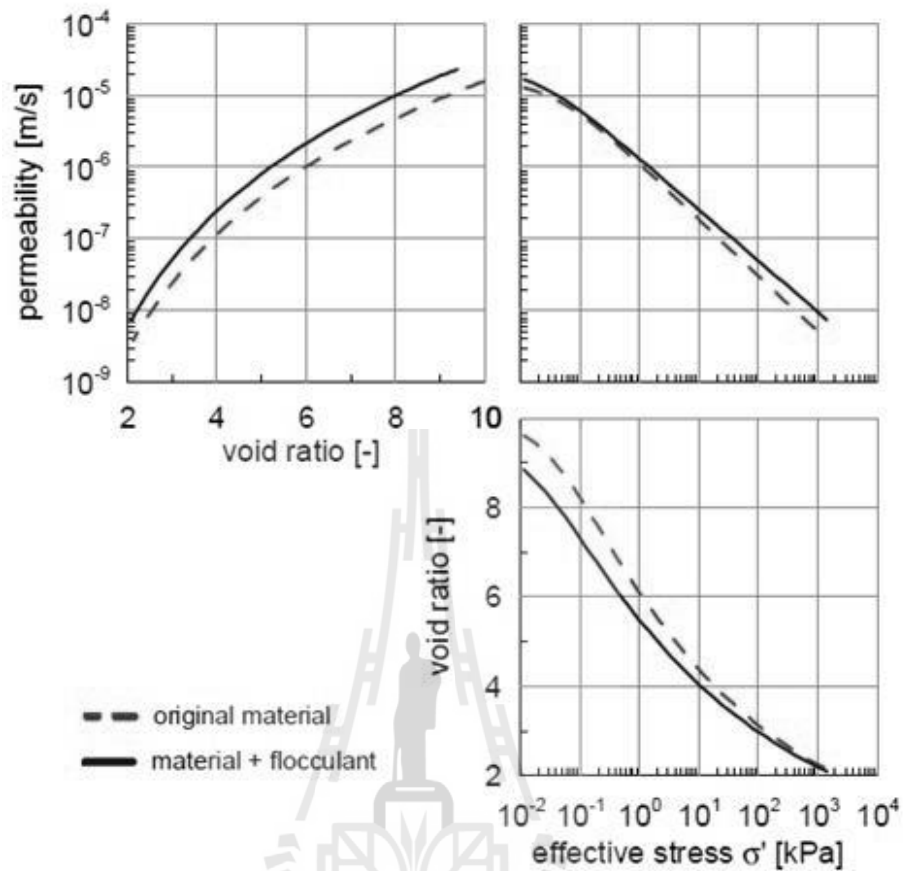


Figure 2.6 Typical result of the impact of flocculant on the large consolidation parameters (Van Impe et al., 2009).

Somtong et al. (2013) determines the mechanical and hydraulic performance of consolidated crushed salt. The brine content is 5% by weight. The samples are consolidated for 3, 5, 7, 10 and 15 days with applied constant axial stresses of 2.5, 5, 7.5 and 10 MPa. The consolidation magnitude and density increase with the applied axial stress. The uniaxial compressive strength increases with the consolidation. The porosity and intrinsic permeability decrease as the consolidation increase.

2.3 Compaction Test

Fuenkajorn and Daemen (1988) study the compressive strength of rock salt from Permian basin, New Mexico. The results are 18.44 MPa of compressive strength, 36 degrees of internal friction angle, 3.42 GPa of tangent modulus, and 5.13 GPa of secant modulus. The salt tends to behave as brittle material (strain-softening) when it is subjected to high strain rates and as ductile material (strain-hardening) for lower strain rates. The sample volume tends to decrease at the beginning of loading and it starts increasing shortly before the peak stress has been reached. The rheological models describe the mechanical behavior of salt but ignore the actual mechanisms of deformation. The deformational characteristics are assumed to be governed by two basic physical elements: spring elasticity and dashpot viscosity. The mechanical behavior of salt is modeled by a combination of these elements. Since the structure of the rheological models is not related to any particular test, the model can be applied to general problems of time-dependent behavior without requiring additional assumptions.

Miao et al. (1995) study constitutive models for healing of materials with application to compaction of crushed rock salt. Crushed rock salt has capability to heal with time. Healing implies that micro cracks and micro voids reduce in size, with corresponding increase strength. Young's modulus and vertical elastic strain.

Ran and Daemen (1995) present results of laboratory compaction testing to determine the influence of particle size, size gradation and moisture content on compaction of crushed rock salt. Included is a theoretical analysis of the optimum size gradation. The objective is to evaluate the relative densities that can be achieved with tamping techniques. Initial results indicate that compaction increases with

maximum particle size and compaction energy, and varies significantly with particle size gradation and water content until the optimum water content is reached (5%), and decreases with further water content increases (Figure 2.7).

Stormont and Finley (1996) present the effective sealing of penetration (borehole) in geological materials. Rock salt formation has naturally low permeability, which make them idea locations for seal in borehole. Furthermore, rock salt has unique properties and behaviors (creep, healing and reconsolidation) which allow the construction of seals which may be effective for very long periods of time. The advantages of crushed salt are the available, low cost, low permeability and obvious compatibility with host rock.

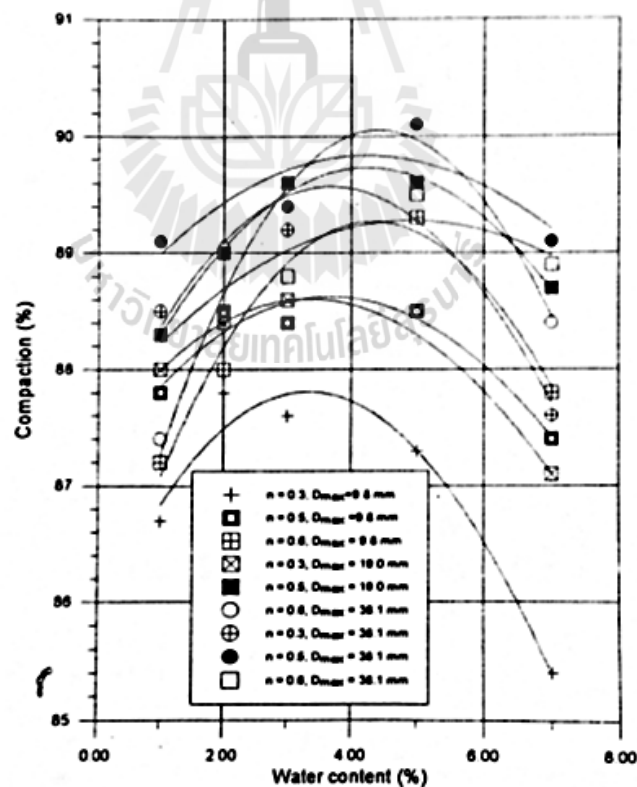


Figure 2.7 Compaction as a function of water content and particle size gradation (Ran and Deamen, 1995).

Hansen (1997) study the brine permeability and mechanical properties on dynamically compacted crushed salt. The results from brine permeability test indicate that the apparent permeability is found to decrease rapidly from an initial value of about $5 \times 10^{-16} \text{ m}^2$ to zero flow after 10 days. The mechanical results include axial, radial, and volumetric creep strains as a function of time. The sign convention uses positive values for compression. Figure 2.8 plots the creep strains for sample RS/DCCS/1, tested under shear consolidation conditions of $\sigma_1 = 5 \text{ MPa}$ and $\sigma_3 = 1 \text{ MPa}$. Figure 2.9 plots the consolidation results for sample RS/DCCS/3, tested at $\sigma_1 = 6 \text{ MPa}$ and $\sigma_3 = 2 \text{ MPa}$. By comparison, test RS/DCCS/3, at a mean stress of 3.33 MPa, exhibits more volumetric strain than RS/DCCS/1, at a mean stress of 2.33 MPa. The ratio of radial strain rate to axial strain rate appears to be lower in RS/DCCS/3 than in RS/DCCS/1. This observation is consistent with predictions of the constitutive model. Using this testing approach, mechanical behavior can be determined as the consolidating salt aggregate assumes an intact material response. A stress state will be determined where the initial radial strain rate will begin in a positive sense, decrease to zero, and eventually change sign and respond like a fully intact salt sample.

Hansen and Mellegard (2002) study the dynamic compacted crushed salt specimens with a diameter of 100 mm and lengths up to 200 mm were derived from the full scale compaction demonstration and from a laboratory scale dynamic compaction study. Starting material was wetted to moisture contents of nominally 1.6 % by weight. Figure 2.10 plots volumetric strain as a function of time on the primary axis and brine flow as a function of time on the secondary axis. Permeability testing of the dynamically compacted crushed salt provided further evidence that the

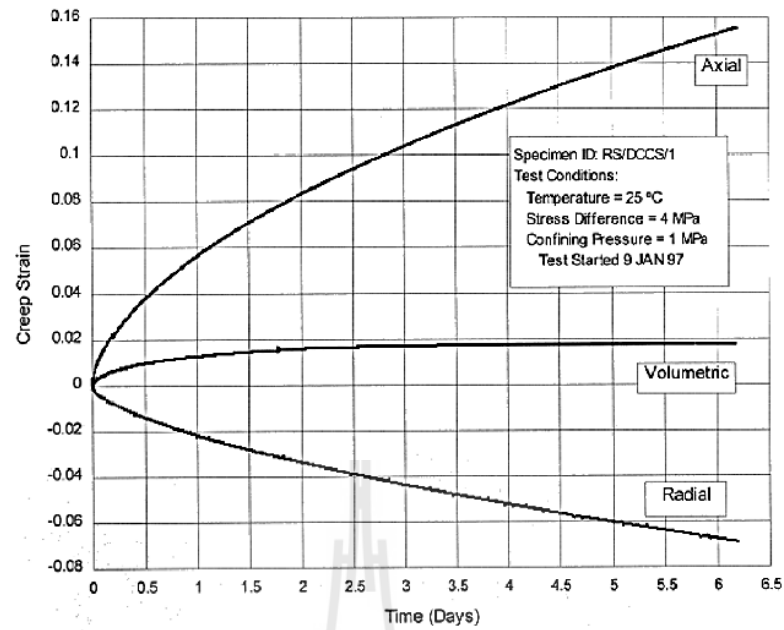


Figure 2.8 Shear consolidations at a mean stress of 2.33 MPa (Hansen, 1997).

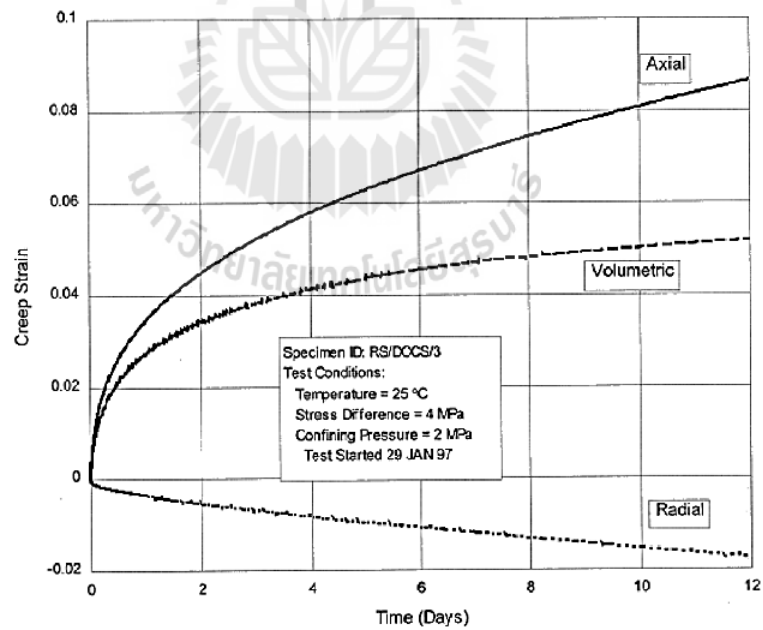


Figure 2.9 Shear consolidations at a mean stress of 3.33 MPa (Hansen, 1997).

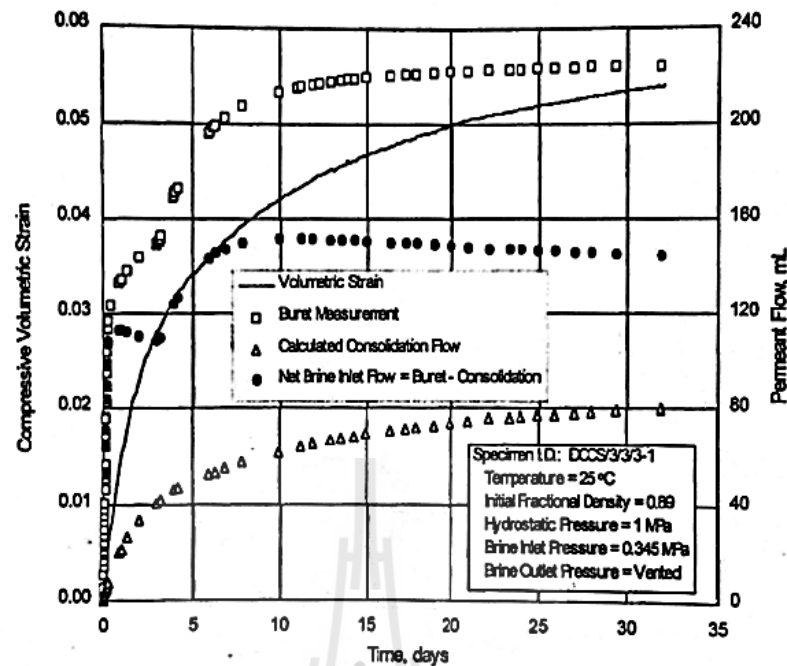


Figure 2.10 Volumetric strain and brine flow as function of time (Hansen and Mellegard, 2002).

permeability decrease as the fraction density of the salt increases. This conclusion agrees with and augments previous results. Shear consolidation creep test results were added to a database of similar results for the purpose of estimating parameter in a constitutive model that represents the behavior of crushed salt (Callahan and Hansen, 1999). Current testing was performed at higher initial fractional densities (0.9) and stresses (1 to 5 MPa) than were used in previous programs to give better coverage of the range of conditions likely to be experienced by salt seal element at the WIPP. The constitutive model predicted that stress states exist where the radial strain rate would initially be positive (consolidation) and then reverse direction and become negative as the specimen density increases. This phenomenon was clearly observed in multiple tests.

Crosby (2007) present the geotechnical properties and geomechanical test results of Maha Sarakham Formation rock type. The overburden consists mainly of mudstone siltstone and sandstone of the Middle Clastic, claystone and mudstone of the Loer clastic, with fractures typically dipping less than 30 degrees, and rarely at 70 degrees. The members are characterized by abundant halite and anhydrite-filled fractures and bands with typical thickness of 2 cm to 5 cm. Direct shear tests perform in this research yield the cohesion and friction angle of 0.30 MPa and 27° for the smooth saw-cut surfaces prepared from the Middle Clastic siltstone.

Fuenkajorn and Phueakphum (2010) performed cyclic loading tests on the Maha Sarakham salt. Their results indicate that the salt compressive strength decreases with increasing number of loading cycles, which can be best represented by a power equation. The salt elastic modulus decreases slightly during the first few cycles, and tends to remain constant until failure. It seems to be independent of the maximum loads. Axial strain–time curves compiled from loci of the maximum load of each cycle apparently show a time-dependent behavior similar to that of creep tests under static loading. In the steady-state creep phase, the visco-plastic coefficients calculated from the cyclic loading test are about an order of magnitude lower than those under static loading. The salt visco-plasticity also decreases with increasing loading frequency. Surface subsidence and cavern closure simulated using parameters calibrated from cyclic loading test results are about 40% greater than those from the static loading results. This suggests that application of the property parameters obtained from the conventional static loading creep test to assess the long-term stability of storage caverns in salt with internal pressure fluctuation may not be conservative.

Samsri et al. (2010) study polyaxial (true triaxial) creep testing has been performed to determine the effect of the intermediate principal stress on the time-dependent behavior of rock salt obtained from the Maha Sarakham formation. A polyaxial creep frame applies constant principal stresses to cubical shaped specimens with a nominal dimension of $5.4 \times 5.4 \times 5.4 \text{ cm}^3$. The applied octahedral shear stresses (τ_{oct}) vary from 5, 8, 11 to 14 MPa while the mean stress (σ_m) is maintained constant at 15 MPa for all specimens. The loading conditions range from the triaxial ($\sigma_1 \neq \sigma_2 = \sigma_3$) to the polyaxial ($\sigma_1 \neq \sigma_2 \neq \sigma_3$ and $\sigma_1 = \sigma_2 \neq \sigma_3$) stress states. The Burgers model is used to describe the elastic, visco-elastic (transient) and visco-plastic (steady-state) behavior of the salt. The specimen deformations are monitored along the three principal axes for up to 21 days. Regression analyses on the octahedral shear strain - time curves suggest that the salt elastic modulus tends to be independent of the intermediate principal stress (σ_2). It however tends to increase as the applied τ_{oct} increases. Under the same magnitude of τ_{oct} the visco-elastic and visco-plastic parameters increase when σ_2 increases from the triaxial condition, $\sigma_2 = \sigma_3$, to the condition where $\sigma_2 = \sigma_1$.

Sriapai et al. (2012) present modified point load (MPL) testing technique is proposed to assess the time dependent properties of rock salt. The Middle and Lower salt members of the Maha Sarakham formation are prepared to obtain rock disk specimens with diameters of 48 and 101mm. These loading platens apply constant axial loads to the circular disk specimens. The induced axial deformation is monitored for various applied axial stresses up to 30 days or until failure occurs. The

elastic and creep parameters obtained from the MPL creep testing and the triaxial creep testing are similar.

2.4 Numerical model

Wagner et al. (1990) present the numerical calculations of disposal room configurations at the Waste Isolation Pilot Plant (WIPP) near Carlsbad, NM are presented. Specifically, the behavior of either crushed salt or a crushed salt-bentonite mixture, when used as a backfill material in disposal rooms, is modeled in conjunction with the creep behavior of the surrounding intact salt. The backfill consolidation model developed at Sandia National Laboratories was implemented into the SPECTROM-32 finite element program. This model includes nonlinear elastic as well as deviatoric and volumetric creep components. Parameters for the models were determined from laboratory tests with deviatoric and hydrostatic loadings. The performance of the intact salt creep model previously implemented into SPECTROM-32 is well documented.

Development of the creep consolidation constitutive equation used in SPECTROM-32 was guided by general consideration with specific functional forms taken from empirical relations matched to available laboratories data. Two continuum internal variables were assumed, the average inelastic volumetric strain, ϵ_{eq1}^c and the average equivalent inelastic shear strain, ϵ_{eq2}^c

$$\dot{\epsilon}_{ij}^c = \dot{\epsilon}_{eq1}^c \frac{\partial \sigma_{eq1}^f}{\partial \sigma_{ij}} + \dot{\epsilon}_{eq2}^c \frac{\partial \sigma_{eq2}^f}{\partial \sigma_{ij}} \quad (2.6)$$

$$\boldsymbol{\varepsilon}_{\text{eq1}}^{\text{c}} = \boldsymbol{\varepsilon}_{\text{v}}^{\text{c}}(\sigma_{\text{m}}) \quad (2.7)$$

$$\boldsymbol{\varepsilon}_{\text{v}}^{\text{c}} = \frac{(1 + \boldsymbol{\varepsilon}_{\text{v}})^2}{\rho_0} B_0 \left[1 - e^{-b_1 \sigma_{\text{m}}} \right] e^{\frac{A \rho_0}{1 + \boldsymbol{\varepsilon}_{\text{v}}}} \quad (2.8)$$

where $\boldsymbol{\varepsilon}_{\text{v}} = \boldsymbol{\varepsilon}_{\text{kk}}$, total volumetric strain, $\boldsymbol{\varepsilon}_{\text{v}}^{\text{c}} = \boldsymbol{\varepsilon}_{\text{kk}}^{\text{c}}$, volumetric creep strain, $\sigma_{\text{m}} = \frac{\boldsymbol{\varepsilon}_{\text{kk}}}{3}$, mean stress, $\rho_0 =$ initial density and $B_0, B_1, A =$ material constants.

Results from the SPECTROM-32 analyses were compared to a similar study conducted by Sandia National Laboratories using the SANCHO finite element program. The calculated deformations and stresses from the SPECTROM-32 and SANCHO analyses agree reasonably well despite differences in constitutive models and modeling methodology. These results provide estimates of the backfill consolidation through time. The trends in the backfill consolidation can then be used to estimate the permeability of the backfill and subsequent radionuclide transport.

Zeuch (1990). The modified Zeuch model (dislocation mechanisms) is based on work performed on dry crushed salt. The modified Spiers model (diffusional transport mechanisms) is based on work performed on wet crushed salt. A comprehensive model should be developed that includes contributions from both types of densification mechanisms. In essence, the modified Zeuch model and the modified Spiers model should be combined or, alternatively, the diffusional process could be added to the modified Zeuch model as outlined by The initial strain rates predicted by both the modified Zeuch and Spiers models are very sensitive to the selection of the starting conditions, which need to be better defined. The initial transient behavior of the crushed salt is not captured very well for higher initial

densities. This could potentially be improved by describing the transient behavior similar to the model used for intact salt.

Itasca (1992) study computer model for describe the rock salt behavior. The finite difference method is well suited to solving problems involving inhomogeneous, complicated geometry, and non-linear material properties. The FDM is a method for approximating derivatives in the equations of motion. Continuous derivatives in differential equations are replaced by finite difference approximations at a discrete set of points in space and time. The resulting set of equations, with 34 appropriate restrictions, can then be solved by algebraic methods. A finite difference model is one, which employs finite difference methods. The resolution of a finite difference model is determined by the spacing of the discrete set of points (grid points) used to approximate the derivatives. The FDM is applied for modeling geomechanical problems that consist of several stages, such as sequential excavation, backfilling and loading.

Callahan and Loken (1996) develop the constitutive models to describe the deformation of crushed salt. The candidate constitutive models are generalized to three-dimensional states of stress to include the effects of mean and deviatoric stress and modified to include the effects of temperature, grain size, and moisture content. A database including hydrostatic consolidation and shear consolidation tests conducted on Waste Isolation Pilot Plant (WIPP) and southeastern New Mexico salt is used to determine material parameters for the candidate constitutive models.

The total strain rate for the crushed-salt constitutive model is assumed to consist of three components. The components include nonlinear elastic (ϵ_{ij}^e),

consolidation (ε_{ij}^c), and creep (ε_{ij}^i) contributions, and the total strain rate is written as the sum of these rates:

$$\varepsilon_{ij} = \varepsilon_{ij}^e + \varepsilon_{ij}^c + \varepsilon_{ij}^i \quad (2.9)$$

Both the nonlinear elastic and consolidation portions of the model describe the material behavior in bulk (volumetric) and in shear (deviatoric).

Following the approach of Fossum et al. (1988), the three-dimensional generalization of the kinetic equation for the consolidation inelastic flow is:

$$\varepsilon_{ij}^c = \varepsilon_{eq}^c (\sigma_{eq}^f) (\partial \sigma_{eq} / \partial \sigma_{ij}) \quad (2.10)$$

where ε_{ij}^c is the inelastic strain rate tensor and σ_{eq}^f and ε_{eq}^c are the power-conjugate equivalent stress measure and equivalent inelastic strain rate measure for creep consolidation, respectively.

The effects of moisture, particle size and temperature are combined to form parameter (ξ), which is incorporated as a multiplicative constant on the equivalent inelastic strain rate:

$$\xi = (L/d^p) [1+a_1 (1- \exp (-a_2w))] \exp (-Q_c/RT) \quad (2.11)$$

where: w = moisture fraction by weight, a_1 , a_2 = material parameters, d = average grain diameter [m], p = material parameter, L = dimensional parameter [m^p], R = universal gas constant [J/(mol-K)], T = absolute temperature [K] and Q_c = material parameter [J/mol].

Three models were selected for evaluation; i.e, those attributed to Sjaardema-Krieg, Zeuch, and Spiers. The models were generalized to three-dimensional forms and modified where deemed necessary. A database comprised of hydrostatic and shear consolidation tests was created and used to determine the material parameters of the candidate constitutive models. Rank ordering of the statistical measures obtained from the model fitting indicates that the modified Spiers model is moderately superior to the other two models. The new stress dependence and generalization enable the models to represent crushed salt behavior under deviatoric stresses.

2.5 Rock salt in northeast region of Thailand

The Department of Mineral Resource had drilled 194 drilled holes between 1976 and 1977 for the exploration of potash (Japakasetr and Suwanich, 1977; Suwanich et al., 1982; Japakasetr, 1985; Suwanich and Ratanajaruraks, 1986). Some boreholes are drilled into the Khok Kruat Formation. The sequences of rock layer from the bottom of this formation up to the top of the Maha Sarakham Formation are as follows:

- 1) Red bed sandstone or dense greenish gray siltstone sometime intercalated with reddish-brown shale;
- 2) Basal anhydrite with white to grey color, dense, lies beneath the lower rock salt and lies on the underlying Khok Kruat formation;
- 3) Lower rock salt the thickest and cleanest rock salt layer, except in the lower part which contains organic substance. The thickness exceeds 400 m in some area and formed salt domes with the thickness as high as 1,000 m, the average thickness is 134 m;

- 4) Potash, 3 types were found; carnallite ($\text{KCl}\cdot\text{MgCl}_2\cdot 6\text{H}_2\text{O}$) with orange, red and pink color, sylvinite (KCl) rarely found, white and pale orange color, an alteration of carnallite around salt domes, and techydrate ($\text{CaCl}_2\cdot 2\text{MgCl}_2\cdot 12\text{H}_2\text{O}$) often found and mixed with carnallite, orange to yellow color caused by magnesium, the dissolved mineral occurred in place.
- 5) Rock salt, thin layers with average thickness of 3 meters, red, orange, brown, gray and clear white colors.
- 6) Lower clastic, clay and shale, relatively pale reddish-brown color and mixed with salt ore and carnallite ore.
- 7) Middle salt, argillaceous salt, pale brown to smoky color, thicker than the upper salt layer with average thickness of 70 meters, carnallite and sylvite may be found at the bottom part.
- 8) Middle clastic, clay and shale, relatively pale reddish brown color and intercalated with white gypsum.
- 9) Upper salt, dirty, mixed with carbon sediment, pale brown to smoky color or orange color when mixed with clay and 3 to 65 meters thick.
- 10) Upper anhydrite, thin layer and white to gray color.
- 11) Clay and claystone, reddish brown color, occurrence of siltstone and sandstone in some places, and
- 12) Upper sediment, brownish gray clay and soil in the upper part, and sandy soil and clay mixed with brown, pink and orange sandy soil in the lower part.

CHAPTER III

SAMPLE PREPARATION

3.1 Introduction

This chapter describes basic characteristics and preparations of materials tested in this study. Materials used in this experiment consist of sludge and crushed salt.

3.2 Sludge-Crushed salt mixture preparation

Sludge used here is obtained from Metropolitan Waterworks Authority in Bangkok. They are collected from sludge dewatering plant of Bang Khen Water Treatment Plant. Dried sludge cake is taken out and dried under sunlight. The moisture is removed again in a hot-air oven at 100°C for at least 24 hours or until its weight remains constant (Figure 3.1). The dried sludge is sieved through a mesh no. 40 to obtain grain sizes ranging from 0.001 to 0.047 mm (Figure 3.2). The basic properties of the sludge indicate that liquid limit is 59%, plastic limit is 31%, plastic index is 28% and specific gravity 2.56. The sludge sample are classified according to the Unified Soil Classification System is in the MH (Silt)

Crushed salt used in this study have been obtained from the Lower member of the Maha Sarakham Formation in the Korat basin, northeastern Thailand. They are crushed by hammer mill (2HP-4 POLES, Spec jis c-4004) show in Figure 3.3. The crushed salt is passing through sieve number 4, 8, 18, 40, 60, 100, 140 and 200. The



Figure 3.1 Sludge dried in a hot-air oven at 100°C.



Figure 3.2 Sludge

grains size of crushed salt ranges from 0.075 to 2.35 mm (Figure 3.4). The grain size distribution of the prepared sludge and crushed salt are shown in Figure 3.5.

Saturated brine is prepared by mixed pure salt with distilled water in plastic tank. The proportion of salt to water is about 39% by weight. Specific gravity of the saturated brine (S.G._B) can be calculated by $S.G._B = \rho_{\text{Brine}}/\rho_{\text{H}_2\text{O}}$, where ρ_{Brine} is density of saturated brine (measured with a hydrometer, kg/m^3) and $\rho_{\text{H}_2\text{O}}$ is density of water (kg/m^3) equal to $1,000 \text{ kg/m}^3$.



Figure 3.3 Salt sample crushed by hammer mill.



Figure 3.4 Crushed salt

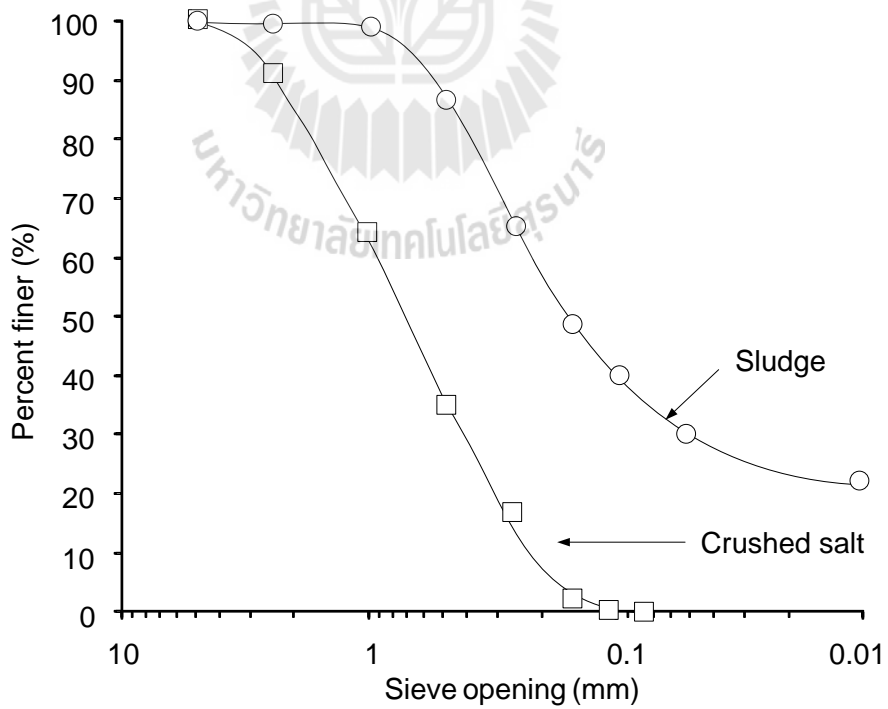


Figure 3.5 Grain size distribution of sludge and crushed salt

3.3 Fabrication of test cylinder

The cylindrical steel tube consists of tube and load platen. The cylindrical tube has 200 mm height, 64 mm outside diameter and 54 mm inside diameter. Two load platens having 53 mm diameter with 100 mm length are used to applied axial load to the sludge-crushed salt mixture specimens. Two o-rings are installed around each load inlet platen to obtain air-tight sealing. There is a 10 mm diameter hole at the center of the top and bottom load platens for use as inlet of N_2 to specimens for permeability testing and drained water from specimen (Figure 3.6).

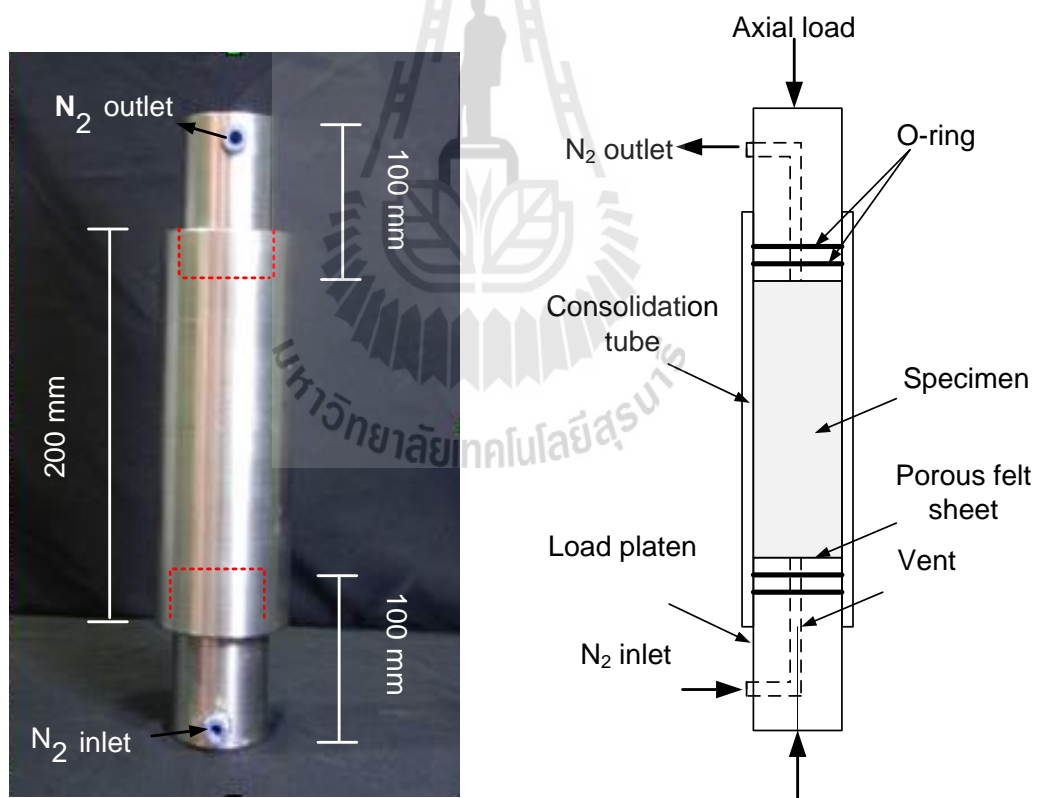


Figure 3.6 Cylindrical steel tubes

CHAPTER IV

LABORATORY TESTING

4.1 Introduction

This chapter describes the methods and results of laboratory experiments used to determine the mechanical and hydraulic properties of sludge-crushed salt mixtures during consolidation as affected by the applied stress and consolidation period.

4.2 Suitable brine content of Sludge

The objectives of these tests are to determine the proportions of optimum saturated brine added to sludge sample. The optimum brine content is determined by applying axial stresses on loading steel piston to the sludge mixed with 2.5, 5, 7.5 and 10% of saturated brine. The axial stress is 2 MPa. All tests are conducted under ambient temperature for 72 hours. Figure 4.1 shows axial strain result measured as a function of time. The results indicate that axial strain increase with increasing brine content. At the 5%, 7.5% and 10% of brine content by weight axial strain are comparable. The proportion of saturated brine to sludge-crushed salt mixture in this study is therefore determined as 5% by weight.

4.3 Consolidation test and results

The consolidation tests are performed by applying constant axial stresses on loading steel piston to the mixture installed in the 54 mm diameter steel cylinder (Figure 4.2). The constant axial stresses of 2.5, 5 and 7.5 MPa and applied for

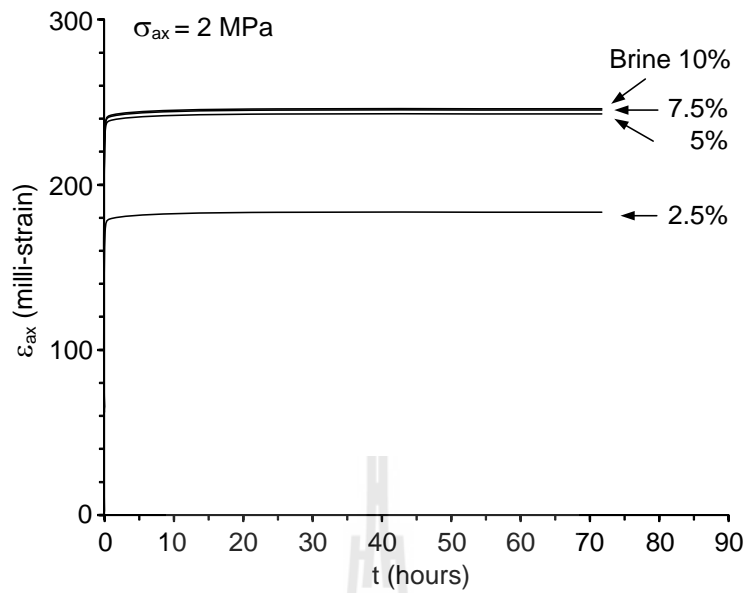


Figure 4.1 Axial strain (ϵ_{ax}) as a function of time (t) for different brine contents.

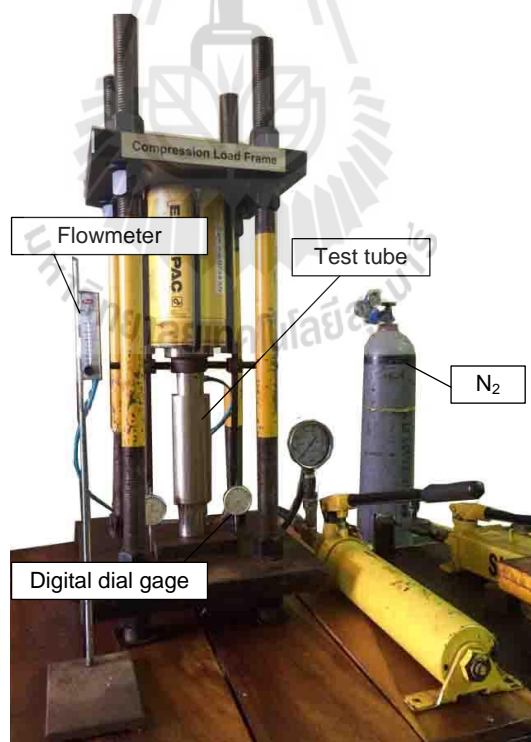


Figure 4.2 Test arrangement for consolidation and permeability testing.

2, 7, 15 and 30 days. All tests are conducted under ambient temperature. The axial displacement is continuously measured as a function of time by dial gage to calculate the change of axial strain.

The consolidation magnitude (axial strains, ε_{ax}) can be calculated using the equation :

$$\varepsilon_{ax} = \Delta L/L \quad (4.1)$$

where ε_{ax} is axial strain of consolidated sludge-crushed salt mixture (mm/mm), ΔL are length change overtime (mm), and L is initial length of the installed specimens.

Results indicate that the volumetric strains of the sludge-crushed salt mixtures increase with axial stresses and consolidation time. The sludge content increase with increasing volumetric strains and sludge content more than 50% is independent with time. Figure 4.3 plot axial strain as a function of time.

4.4 Nitrogen flow test and result

The nitrogen flow testing (Figure 4.4) is performed to determine the intrinsic permeability (k) of the sludge-crushed mixtures during consolidation. The flow rates under constant head are continuously monitored every 6 hours. The nitrogen gas is injected under 20 psi into the steel tube. The outflow rates are monitored using high precision flow-meter. The permeability coefficient can be calculated based on the ASTM (D2434-68): $\Delta h = (\Delta P/\gamma_f)$ where Δh is head difference (m), ΔP is difference pressure at the initial point and end point (kPa), and γ_f is unit weight of gas (kN/m^3). The hydraulic conductivity is obtained from:

$$Q = KA (\Delta h/L) \quad (4.2)$$

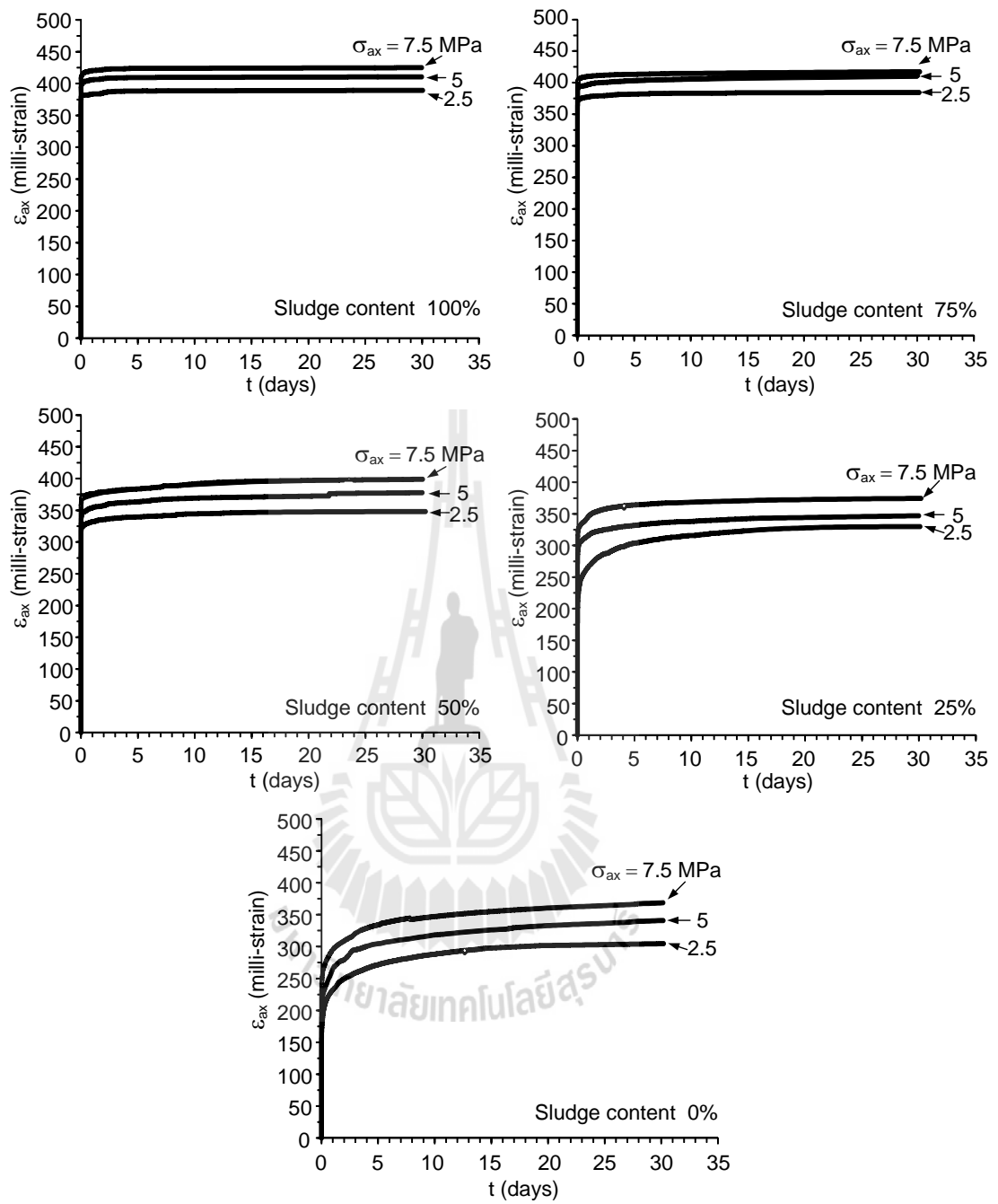


Figure 4.3 Axial strain (ϵ_{ax}) as a function of time (t) for different axial stresses (σ_{ax}).

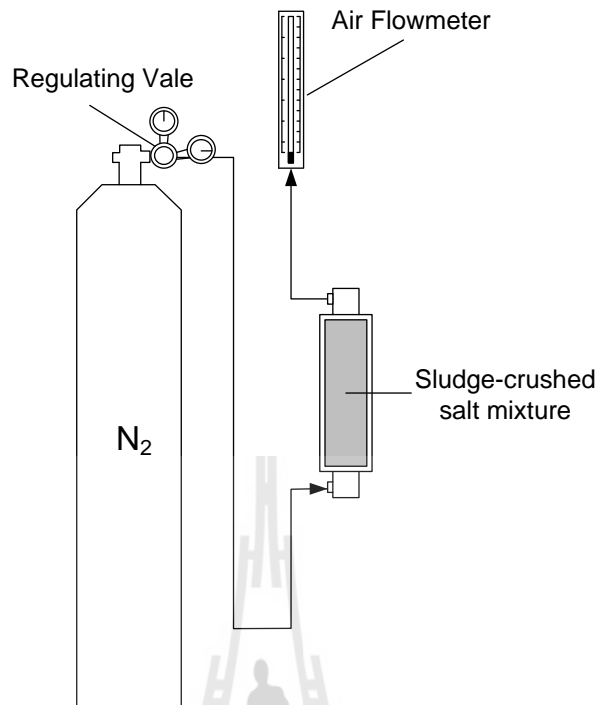


Figure 4.4 Nitrogen gas flow test.

where K is hydraulic conductivity (m/s), Q is flow rate (m^3/s), A is a cross-section area of flow (m^2), $\Delta h/L$ is hydraulic gradient. The hydraulic conductivity is used to calculate the intrinsic permeability (k) by Indraratna and Ranjith (2001):

$$k = (K\mu/\gamma_f) \quad (4.3)$$

where k is intrinsic permeability (m^2), and μ is dynamic viscosity of N_2 ($\text{Pa}\cdot\text{s}$).

The results indicate that when the consolidation time, axial stress and sludge content increase the intrinsic permeability of sludge-crushed salt mixture decreases, as shown in Figure 4.5. The outflow of sludge-crushed salt mixtures at 50:50, 75:25 and 100:0 cannot be detected. The lower limit of the measurement system is 10^{-11} m^2 .

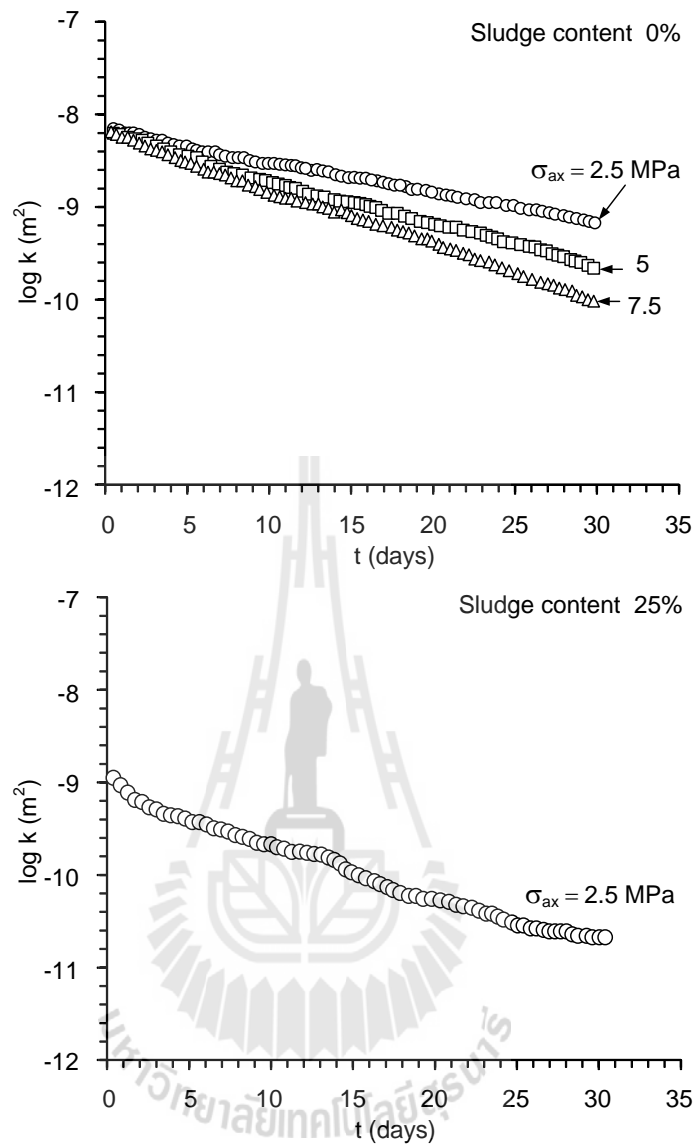


Figure 4.5 Intrinsic permeability (k) as a function of time (t) and for different axial stresses (σ_{ax}).

4.5 Uniaxial compressive strength test and results

The uniaxial compressive strength test procedure follows as much as practical the ASTM (D2938-95) standard practice and the ISRM suggested method. The compressive strength is determined by axially loading the consolidated sludge-

crushed salt mixture cylinder (after removing from the steel tube) with a nominal diameter of 54 mm and L/D ranging 2 to 3 (Figure 4.6) and density decreases with increasing sludge content and increases with axial stress and consolidation time (Figure 4.7). Neoprene sheets are used to minimize the friction at the interfaces between the loading platens and the sample surfaces. The sludge-crushed salt mixture samples are loaded at the constant rate of 0.5-1 MPa/second until failure. The axial and lateral displacement is monitored by dial gages (Figure 7.8). The elastic modulus (E) and Poisson's ratio (ν) are determined from the tangent about 50% of the failure stress. Figure 4.9 shows some post-test specimen of sludge-crushed salt mixture after uniaxial compressive strength testing.

The results indicate that the uniaxial compressive strength and elastic modulus decrease with increasing sludge content and increase with axial stress and consolidation time. The Poisson's ratios decrease with increasing axial stress, sludge content and consolidation time. The results are shown in Figures 4.10 through 4.16.



Figure 4.6 Sludge-crushed salt mixture specimens after consolidation.

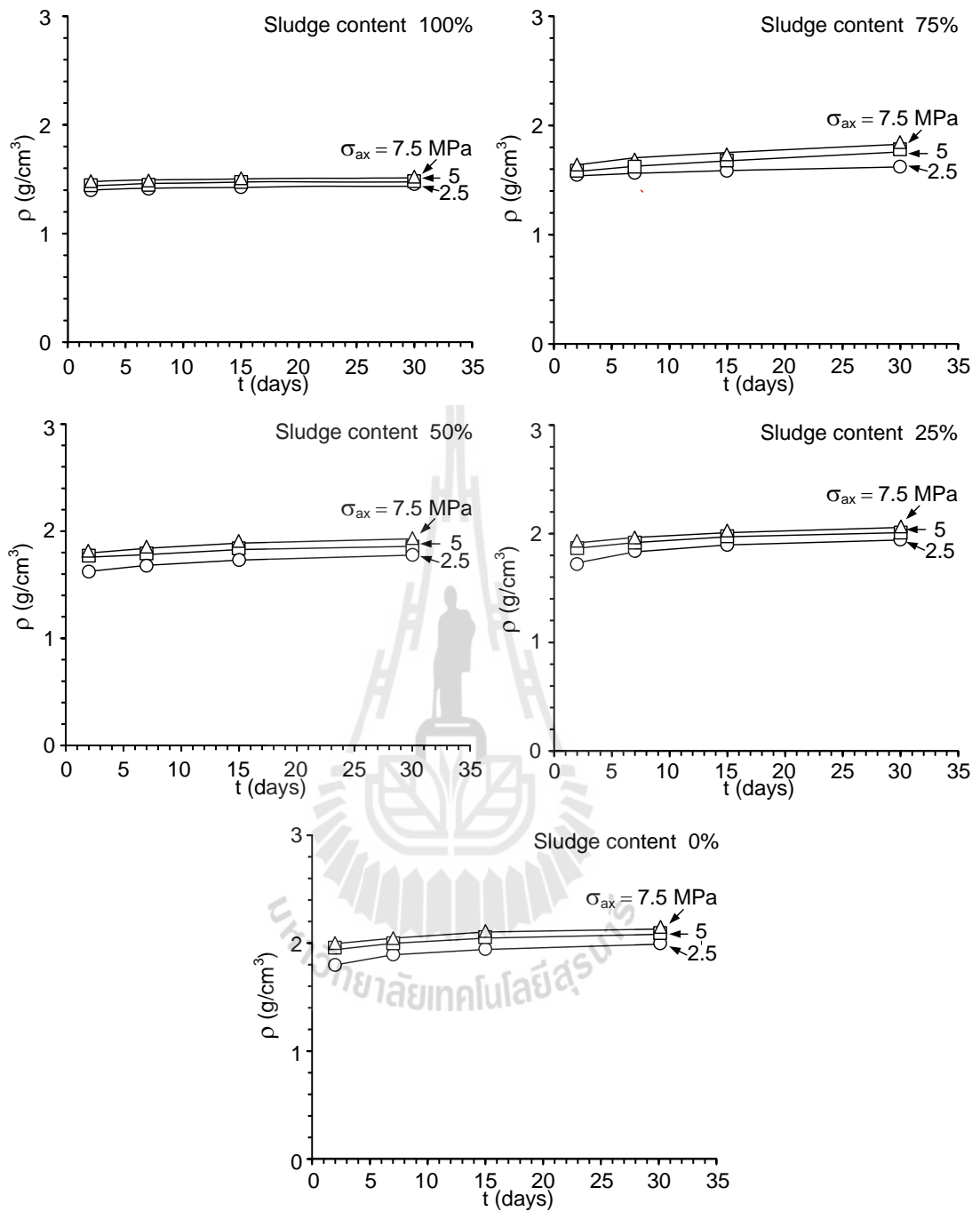


Figure 4.7 Density (ρ) as a function of consolidation time (t) for different consolidation stresses (σ_{ax}).

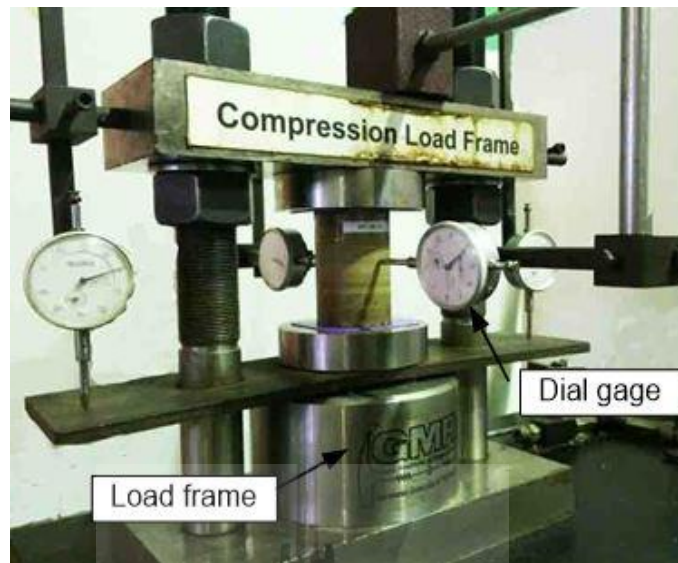


Figure 4.8 Arrangement of uniaxial compressive strength testing.

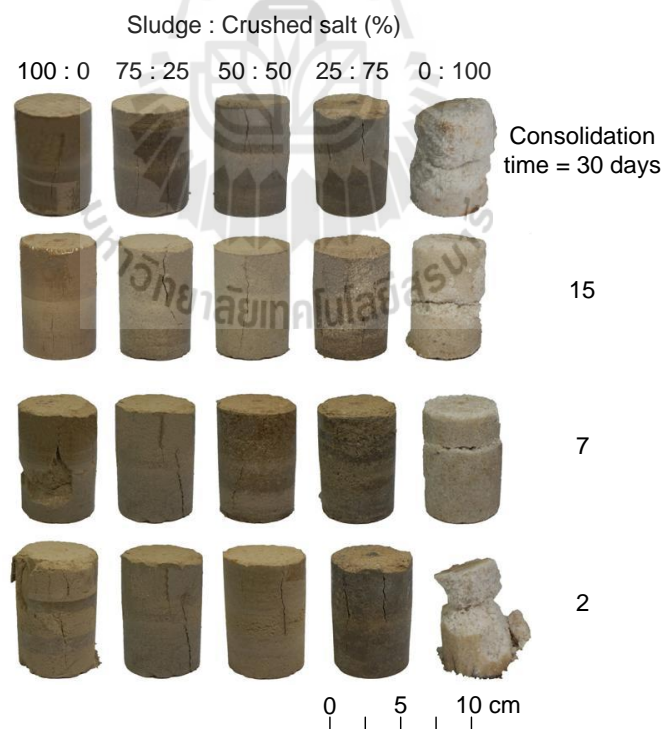


Figure 4.9 Some post-tested sludge-crushed salt mixture specimens after uniaxial compressive strength testing.

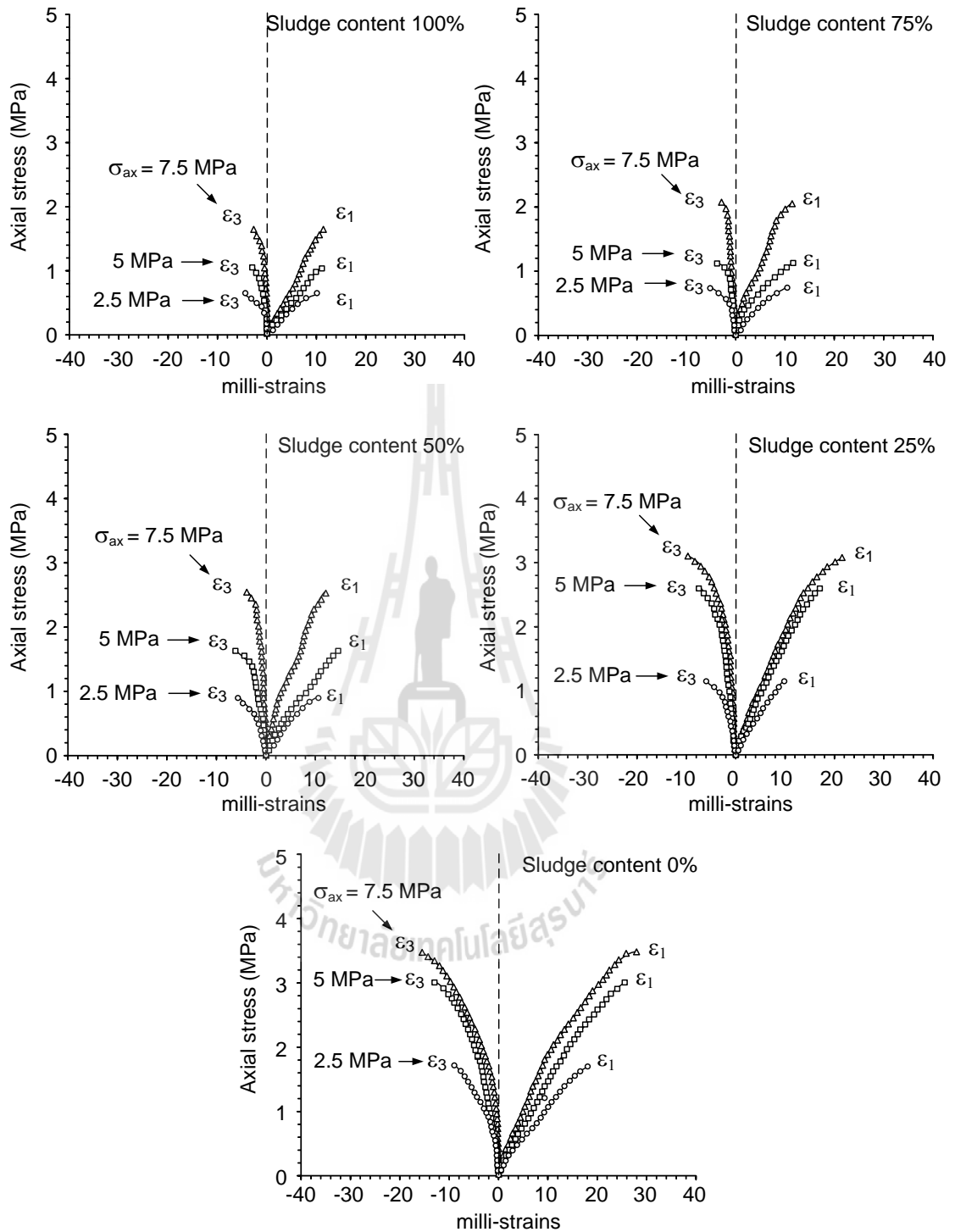


Figure 4.10 Uniaxial stress-strain curves of specimens after 2 days of consolidation.

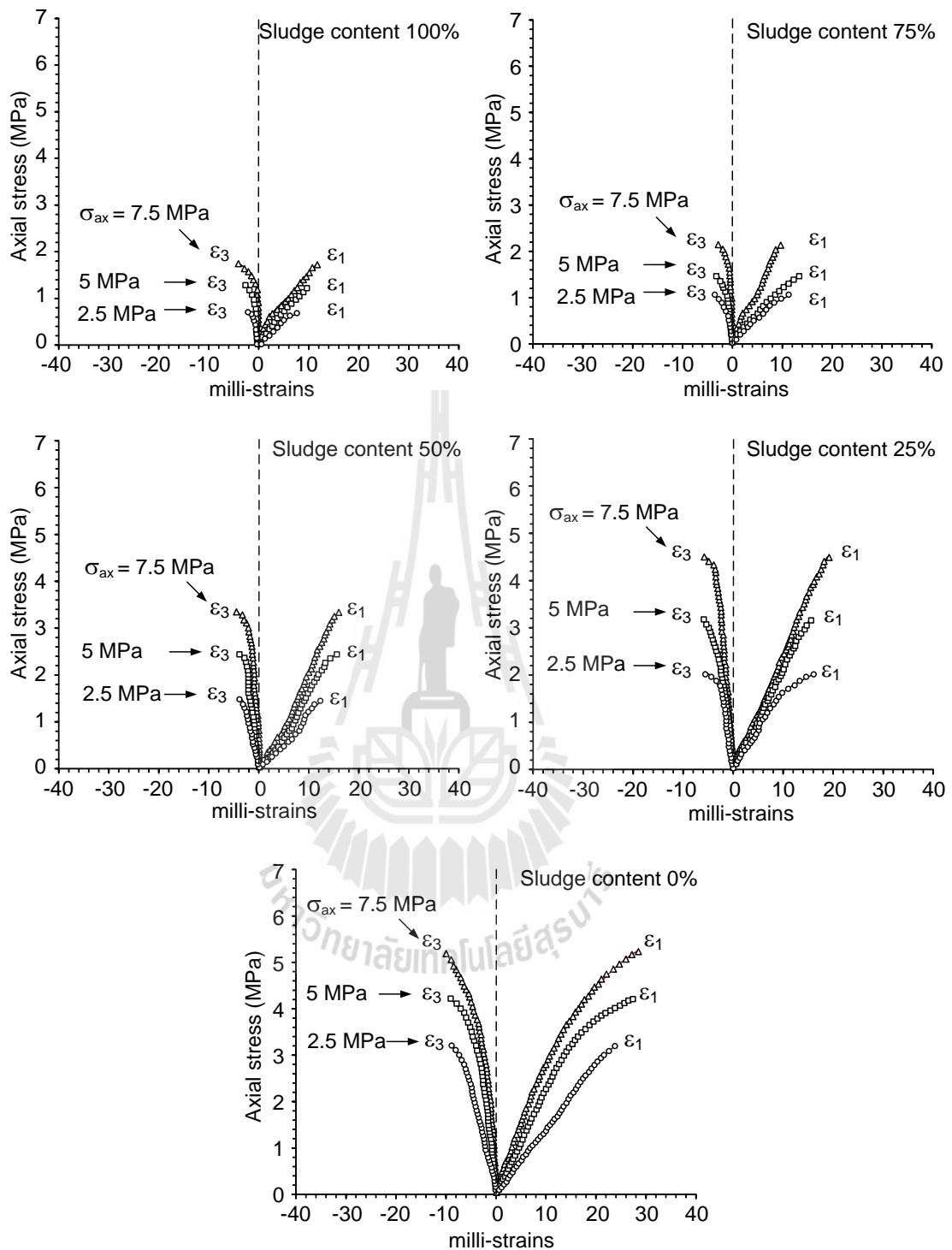


Figure 4.11 Uniaxial stress-strain curves of specimens after 7 days of consolidation.

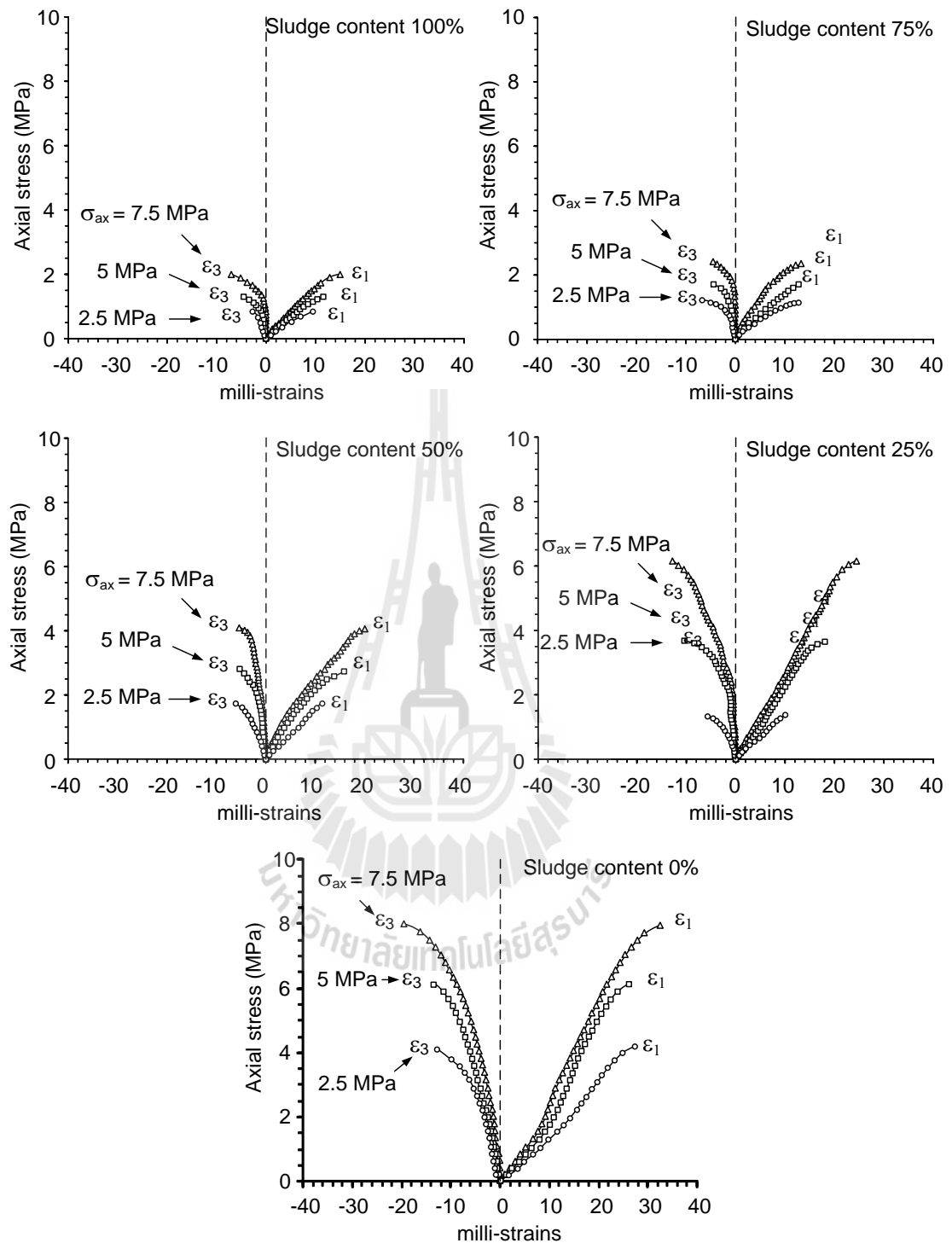


Figure 4.12 Uniaxial stress-strain curves of specimens after 15 days of consolidation.

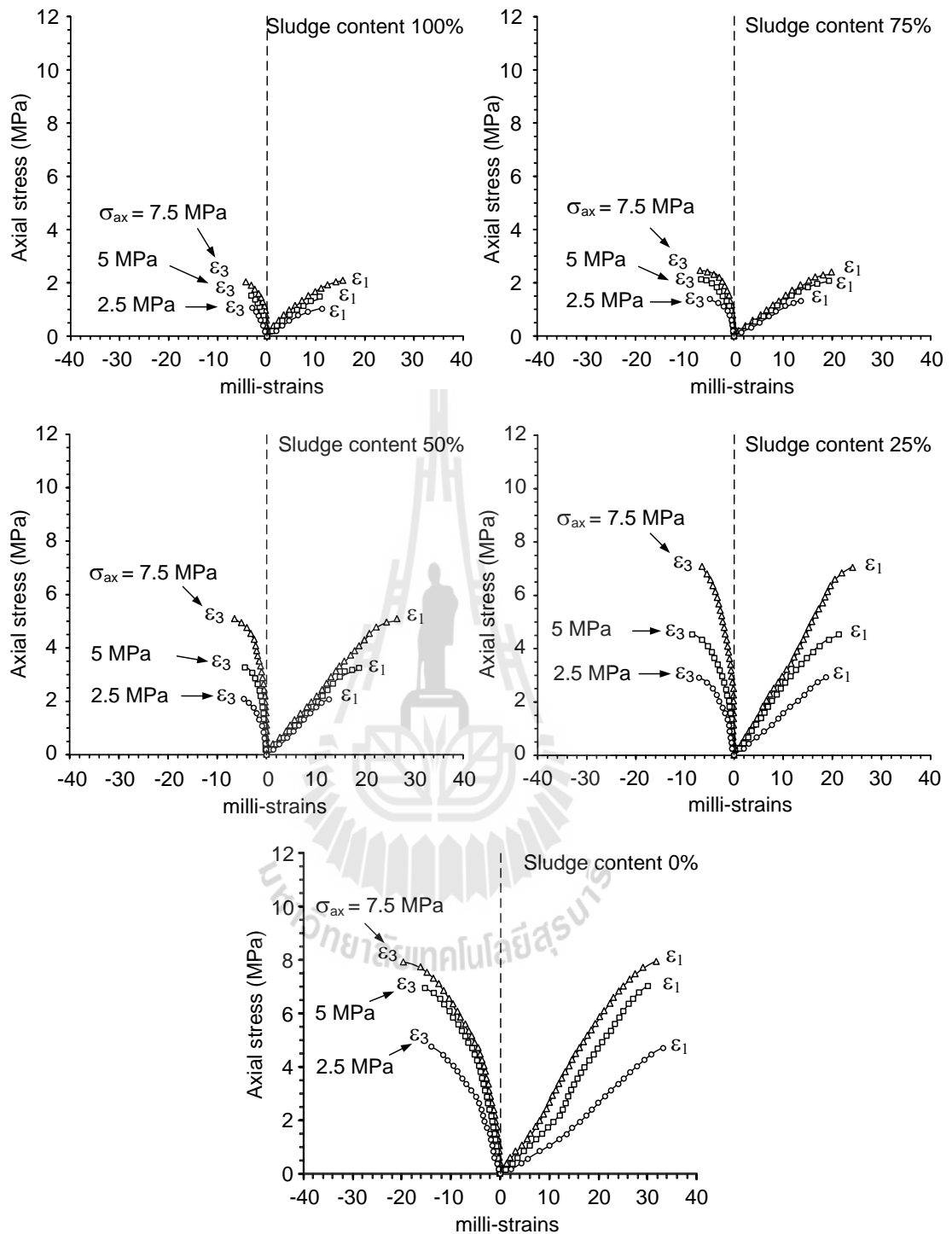


Figure 4.13 Uniaxial stress-strain curves of specimens after 30 days of consolidation.

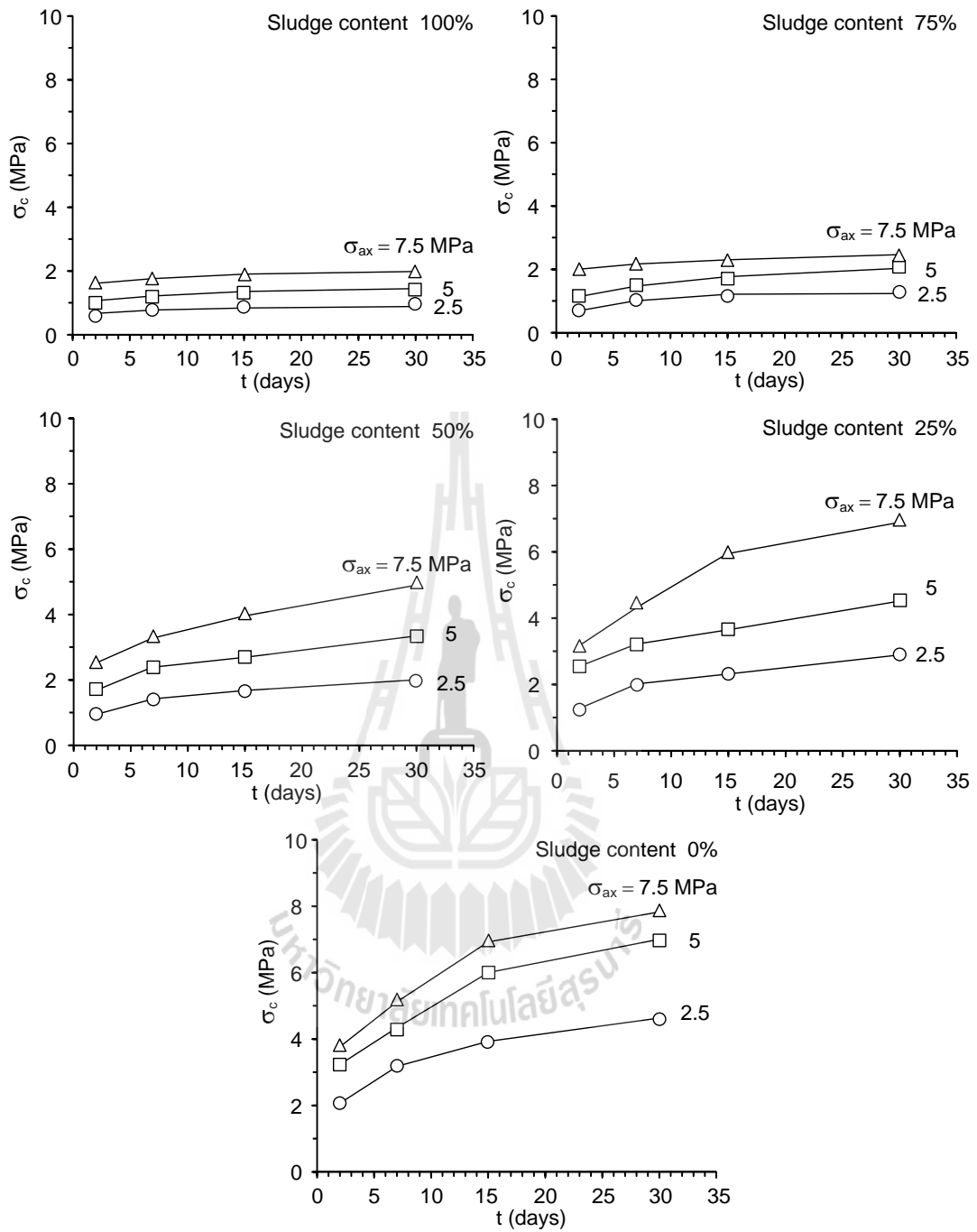


Figure 4.14 Uniaxial compressive strengths (σ_c) as a function of consolidation time (t) for different consolidation stresses (σ_{ax})

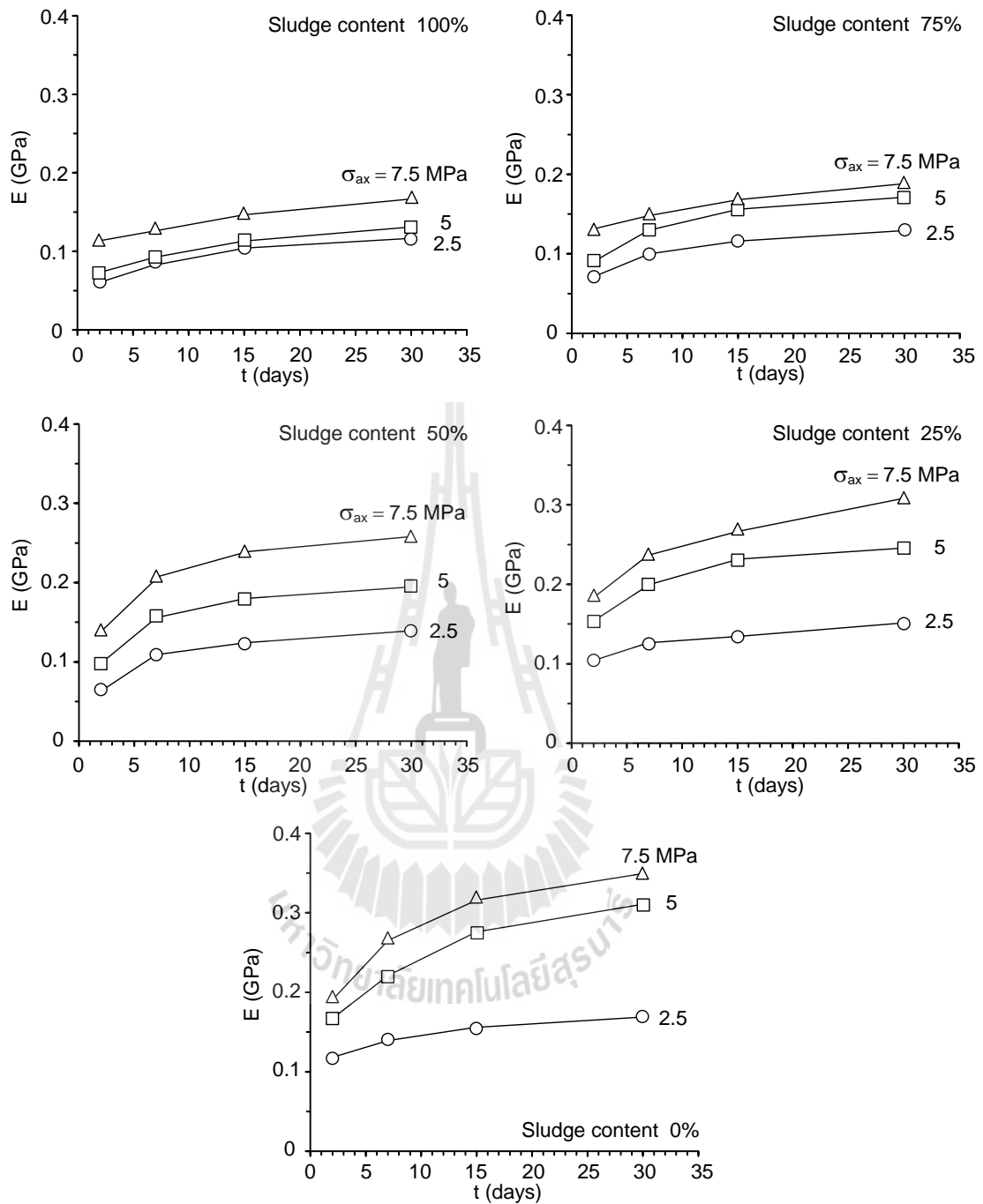


Figure 4.15 Elastic modulus (E) as a function of consolidation time (t) for different consolidation stresses (σ_{ax}).

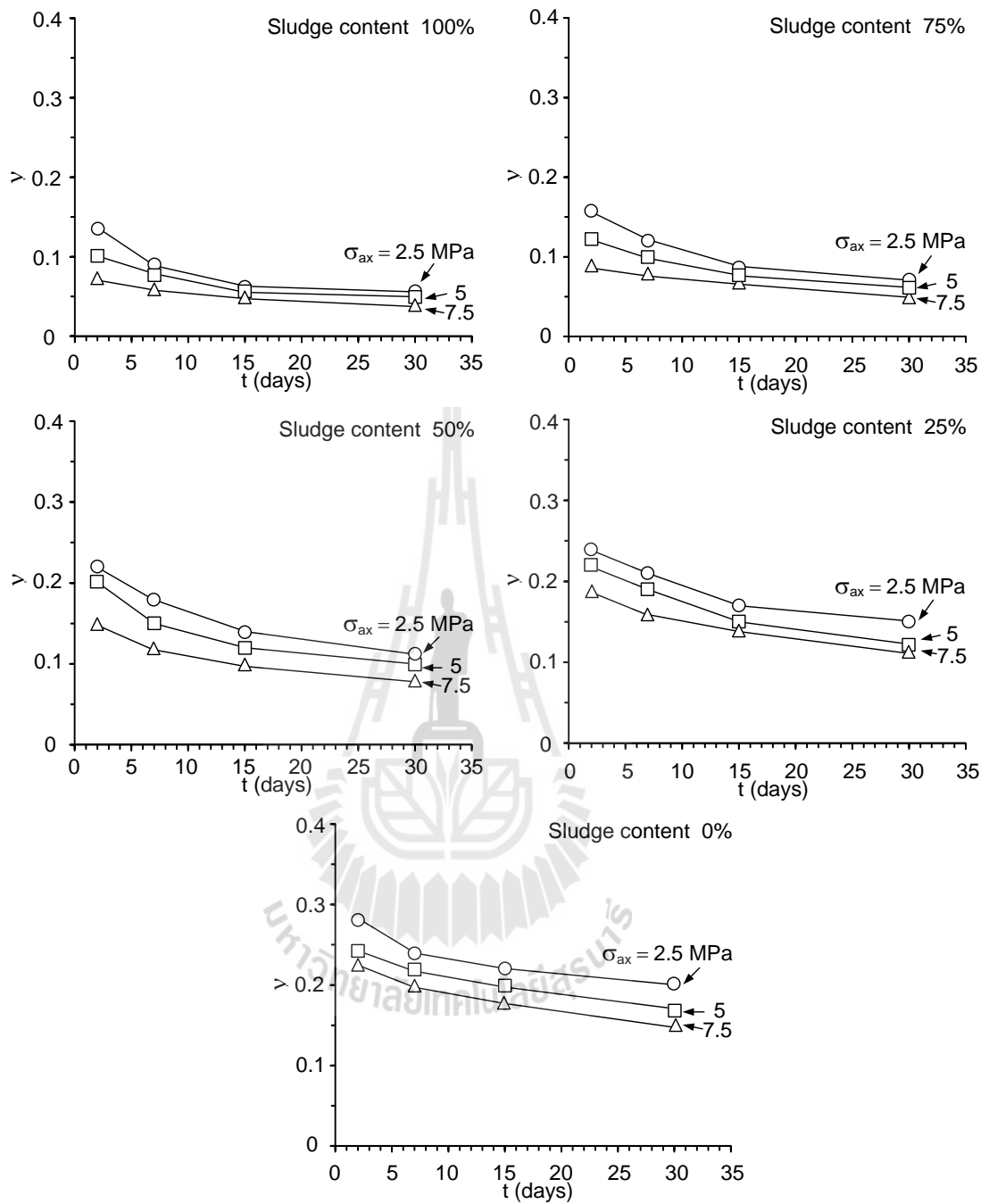


Figure 4.16 Poisson's ratio (ν) as a function of consolidation time (t) for different consolidation stresses (σ_{ax}).

CHAPTER V

DEVELOPMENT OF EMPIRICAL EQUATIONS

5.1 Introduction

The objective of this chapter is to predict the mechanical and hydraulic properties of sludge-crushed salt mixtures for use as backfill material in the mine openings. Sets of mathematical equations derived to link the mean stress with the volumetric strain, intrinsic permeability, uniaxial compressive strength, elastic modulus, Poisson's ratio and density after consolidating under uniaxial strain condition. The regression analysis on the test data using SPSS Statistics 19 (Wendai, 2000) is performed to determine relevant parameters. Such relation will be useful for the determination of the installation parameters for the sludge-crushed salt mixtures in the mine openings.

5.2 Uniaxial strain condition

The empirical equations are calculated based on the uniaxial strain condition ($\varepsilon_1 \neq 0, \varepsilon_2 = \varepsilon_3 = 0, \sigma_2 = \sigma_3 \neq 0$). Poisson's ratio from the uniaxial compressive strength and axial strain is used to calculate the lateral stresses (σ_3) as follows (Jaeger et al., 2007)

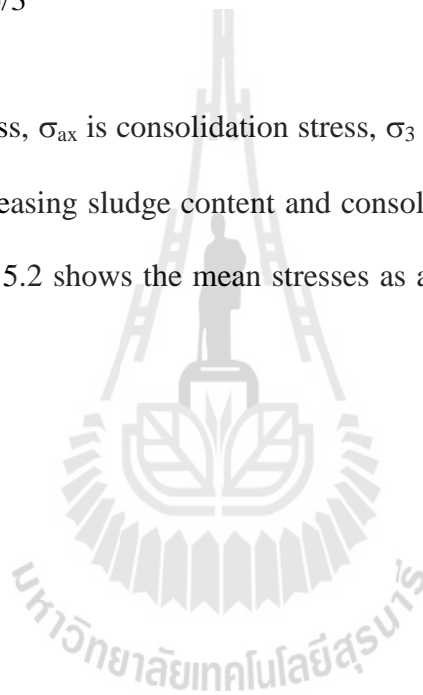
$$\sigma_2 = \sigma_3 = [\nu / (1 - \nu)] \sigma_1 \quad (5.1)$$

where σ_2 and σ_3 are lateral stresses, ν is Poisson's ratio and σ_1 is consolidation

stress (σ_{ax}). The results indicate that the lateral stresses decrease with the increasing sludge content and consolidation time and increase with axial stresses. Figure 5.1 shows the lateral stresses as a function of time for different consolidation stresses. The mean stresses (σ_m) are also determined using the following relations (Jaeger et al., 2007)

$$\sigma_m = (\sigma_{ax} + 2\sigma_3)/3 \quad (5.2)$$

where σ_m is mean stress, σ_{ax} is consolidation stress, σ_3 is lateral stress. Mean stresses decrease with the increasing sludge content and consolidation time and increase with axial stresses. Figure 5.2 shows the mean stresses as a function of time for different applied axial stresses.



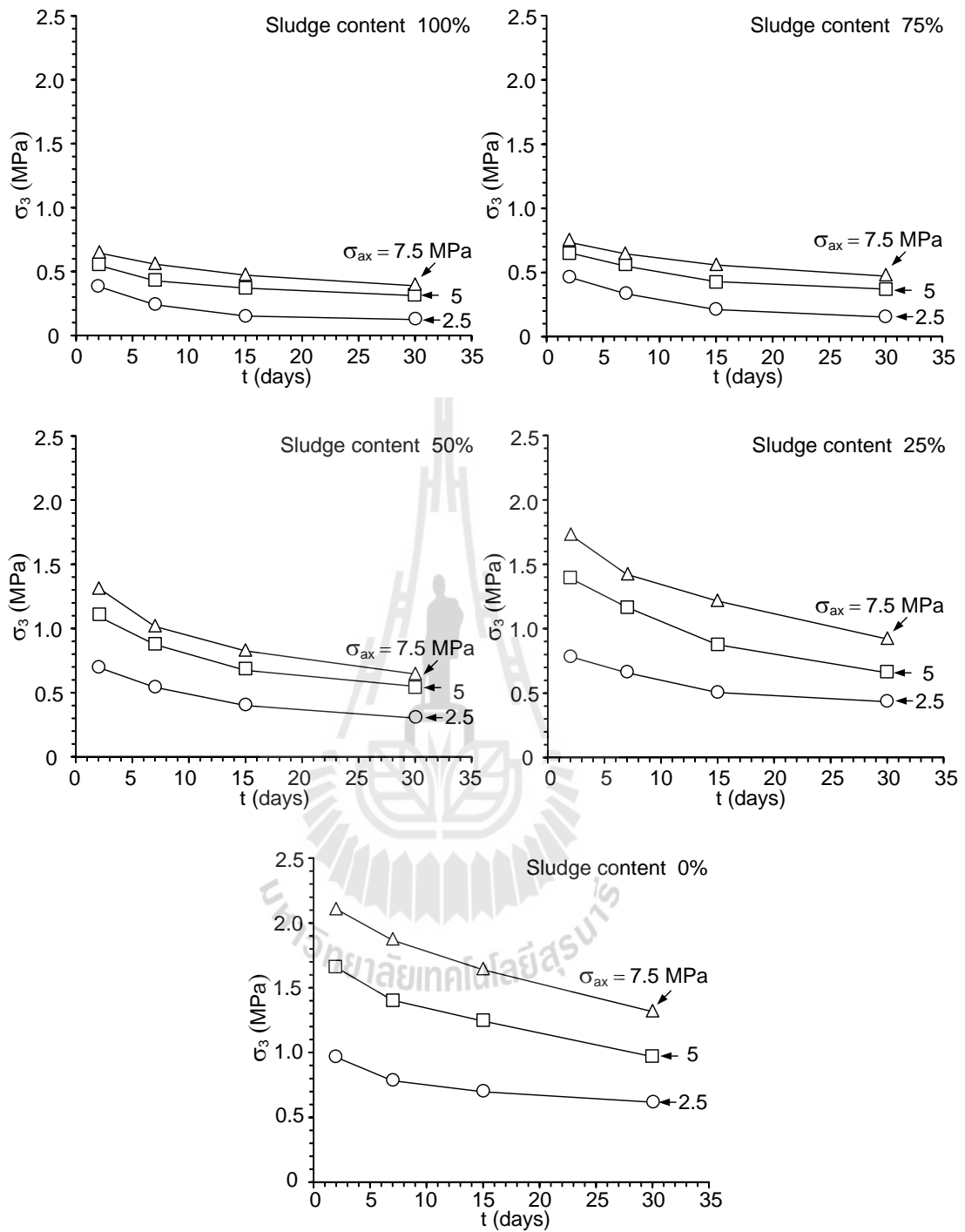


Figure 5.1 Lateral stresses (σ_3) as a function of time (t) for different axial stresses (σ_{ax}).

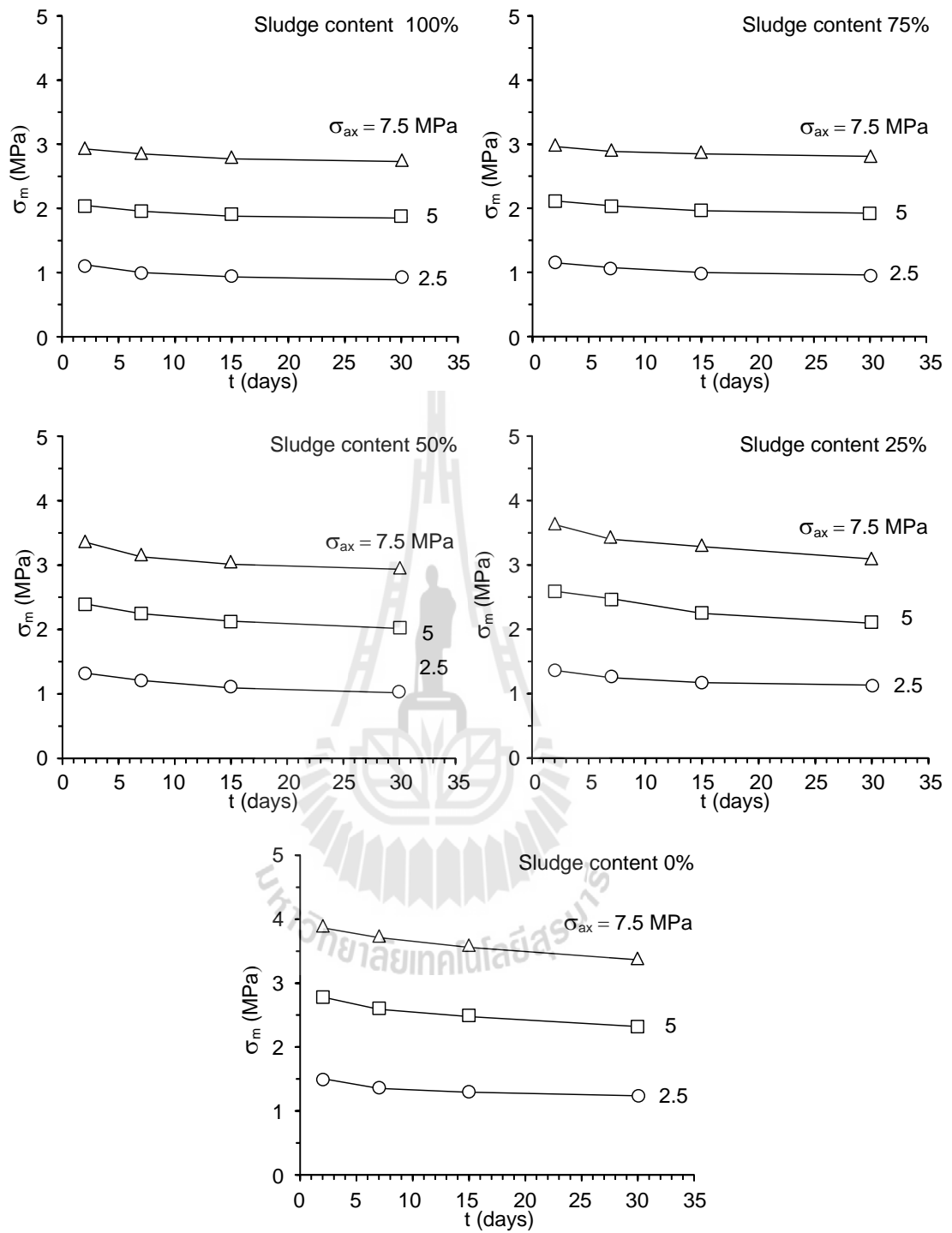


Figure 5.2 Mean stresses (σ_m) as a function of time (t) for different axial stresses (σ_{ax}).

5.3 Empirical equations

5.3.1 Mean stress of sludge-crushed salt mixtures

The test results are used to develop a set of empirical equation as a function of axial stresses and time. The relationships of mean stress and times are non-linear which can be represented by:

$$\sigma_m = (\alpha \cdot t^\beta) + (\delta \cdot \sigma_{ax}) \quad (5.3)$$

where σ_m is mean stress, t is time for consolidation (days), σ_{ax} is consolidation stress, α , β and δ are empirical constants. Regression analysis on the test data using SPSS statistical software can determine these constant (table 5.1). Good correlation ($R^2 = 0.974$ to 0.996) between the proposed empirical constitutive equation and the test data is obtained. Figure 5.3 compares the test data with the back prediction of the proposed equation.



Table 5.1 Parameters of mean stresses relationship

Sludge content by weight (%)	Parameters	Values	Coefficients of correlation
100	α	0.553	0.974
	β	-0.595	
	δ	0.371	
75	α	0.571	0.996
	β	-0.578	
	δ	0.360	
50	α	0.609	0.996
	β	-0.553	
	δ	0.391	
25	α	0.625	0.992
	β	-0.538	
	δ	0.421	
0	α	0.655	0.994
	β	-0.525	
	δ	0.457	

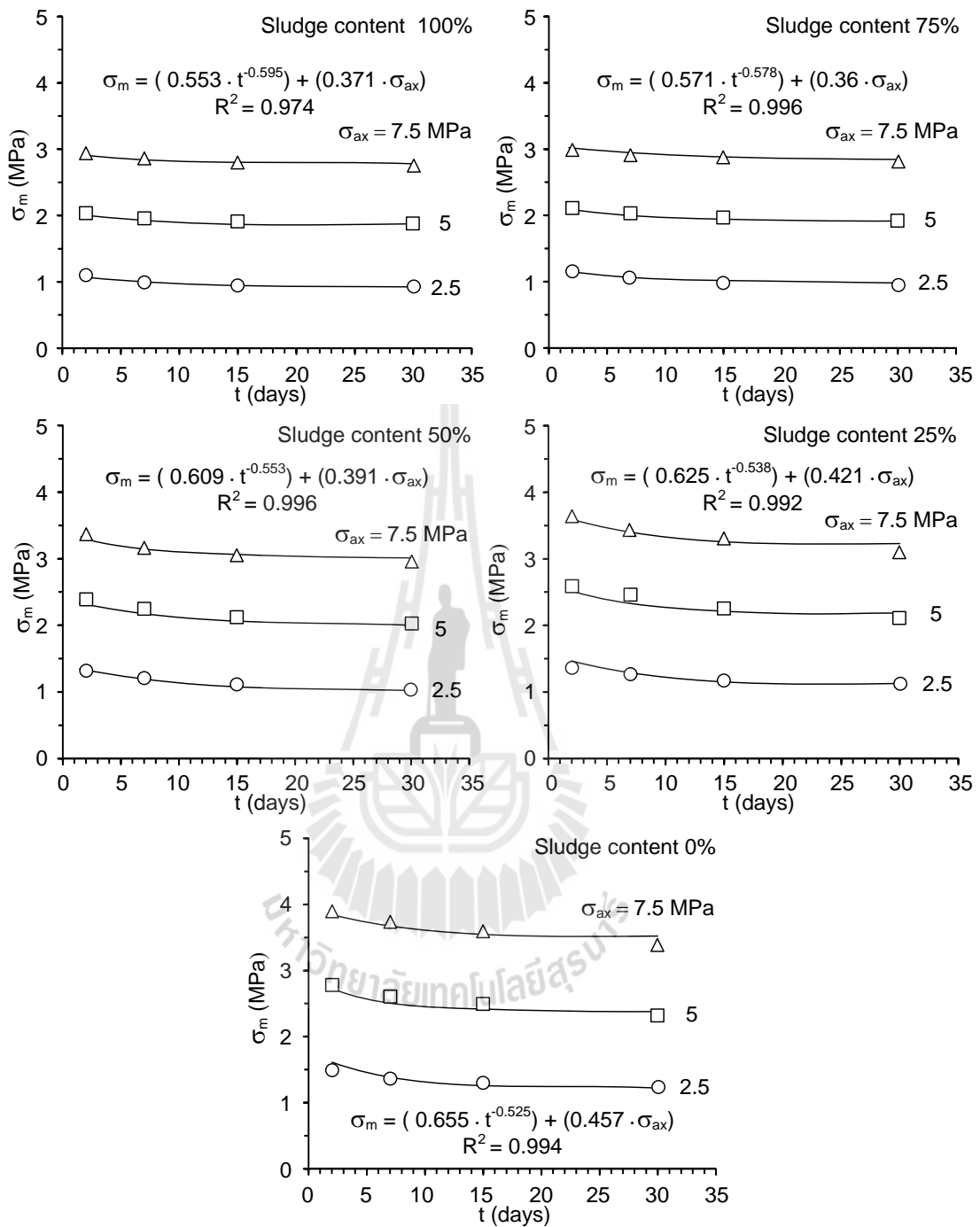


Figure 5.3 Mean stresses (σ_m) as a function of time (t) and axial stresses (σ_{ax}), test result (point) and back prediction (lines).

5.3.2 Volumetric strain of sludge-crushed salt mixture

The axial strains from the measurement results represent the volumetric strain of sludge-crushed salt mixture samples. The volumetric strains increase with the sludge content, axial stresses and consolidation time. The results are used to develop an empirical equation as a function of mean stress and time. The relationships are non-linear which can be represented by:

$$\Delta v/v = \phi \cdot \sigma_m^\gamma \cdot t^\eta \quad (5.4)$$

where $\Delta v/v$ is volumetric strain, σ_m is mean stress (MPa), t is time of consolidation (days), ϕ , γ , and η are empirical constants. The range of obtained coefficients of correlation from the testing is 0.865 to 0.990. The constant parameters are shown in Table 5.2. This equation can be used to predict the volumetric strain at consolidation periods and under mean stress. Figure 5.4 shows the test data with the back prediction of the proposed equation.

Table 5.2 Parameters of volumetric strain relationship

Sludge content by weight (%)	Parameters	Values	Coefficients of correlation
100	ϕ	381.205	0.99
	γ	0.086	
	η	0.007	
75	ϕ	373.049	0.976
	γ	0.081	
	η	0.011	
50	ϕ	314.487	0.989
	γ	0.134	
	η	0.027	
25	ϕ	264.572	0.865
	γ	0.176	
	η	0.049	
0	ϕ	216.921	0.973
	γ	0.205	
	η	0.085	

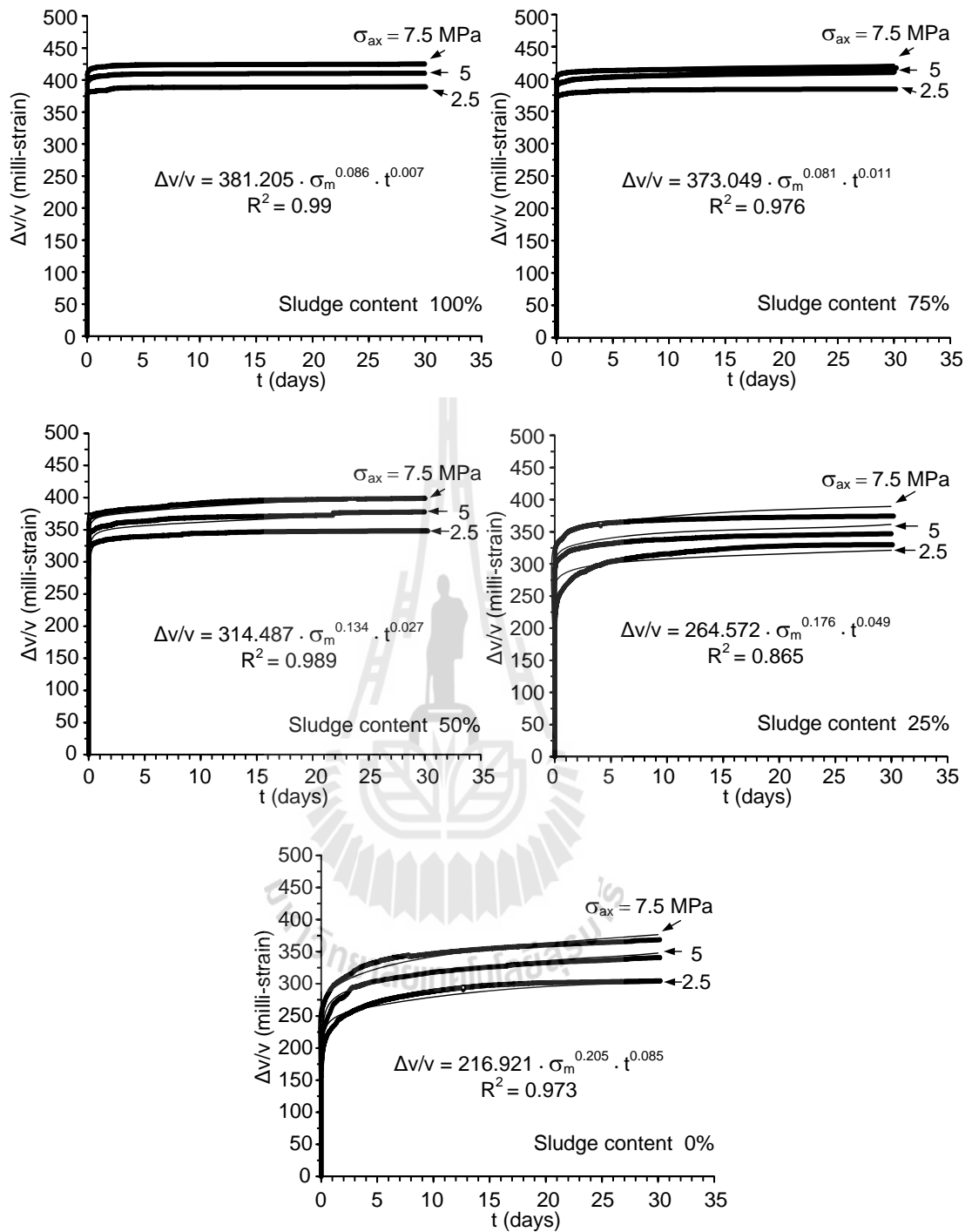


Figure 5.4 Volumetric strain ($\Delta v/v$) as a function of time (t) and mean stresses (σ_m), test result (points) and back prediction (lines).

5.3.3 Permeability of sludge-crushed salt mixture

The intrinsic permeability of the sludge-crushed salt samples decrease with the increasing sludge content, axial stresses and consolidation time. The relationships can be represented by:

$$k = \varphi \cdot \exp(\kappa \cdot \sigma_m \cdot t) \quad (5.5)$$

where k is intrinsic permeability of sludge-crushed salt sample (m^2), σ_m is mean stress (MPa), t is time for consolidation (days), φ and κ are empirical constants. The constant parameters are shown in Table 5.3. The coefficient of correlation from testing is 0.898. This equation can be used to predict the intrinsic permeability occurred at consolidation periods and under mean stress. Figure 5.5 shows the test data with the back prediction of the proposed equation.

Table 5.3 Parameters of intrinsic permeability relationship.

Sludge content by weight (%)	Parameters	Values	Coefficients of correlation
25	φ	7.85×10^{-10}	0.898
	κ	-0.012	
0	φ	6.12×10^{-9}	0.898
	κ	-0.045	

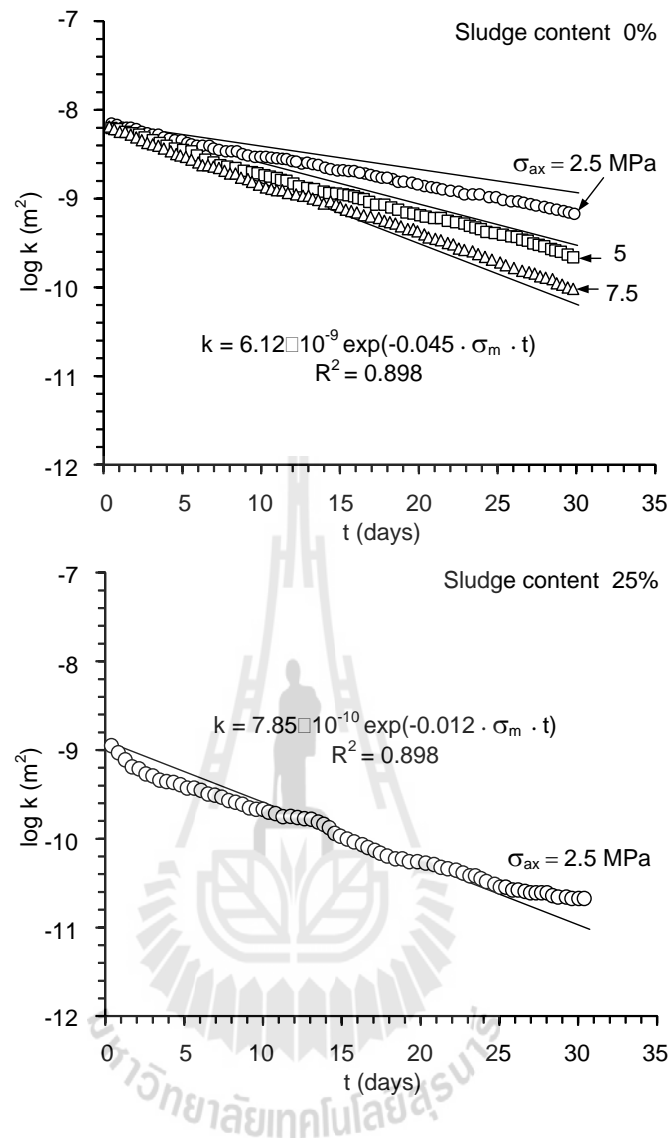


Figure 5.5 Intrinsic permeability (k) as a function of time (t) and mean stresses (σ_m), test result (points) and back prediction (lines).

5.3.4 Density of sludge-crushed salt mixture

Density of the sludge-crushed salt samples increase with the axial stresses and consolidation time and decrease with increasing sludge content. The relationships are can be represented by:

$$\rho = \Omega \cdot \sigma_m^\zeta \cdot t^\iota \quad (5.6)$$

where ρ is density of sludge-crushed salt sample, σ_m is mean stress (MPa), t is time for consolidation (days), Ω , ζ and ι are empirical constants. Table 5.4 shows constant parameters of density relationship. Good correlation ($R^2 = 0.801$ to 0.916) between the proposed equation and the test results is obtained. This equation can be used to predict the density occurred at consolidation times and mean stress. Figure 5.6 shows the test data with the back prediction of the proposed equation.

Table 5.4 Parameters of density relationship.

Sludge content by weight (%)	Parameters	Values	Coefficients of correlation
100	Ω	1.406	0.916
	ζ	0.029	
	ι	0.011	
75	Ω	1.525	0.800
	ζ	0.049	
	ι	0.026	
50	Ω	1.638	0.864
	ζ	0.052	
	ι	0.028	
25	Ω	1.729	0.907
	ζ	0.056	
	ι	0.034	
0	Ω	1.807	0.886
	ζ	0.062	
	ι	0.028	

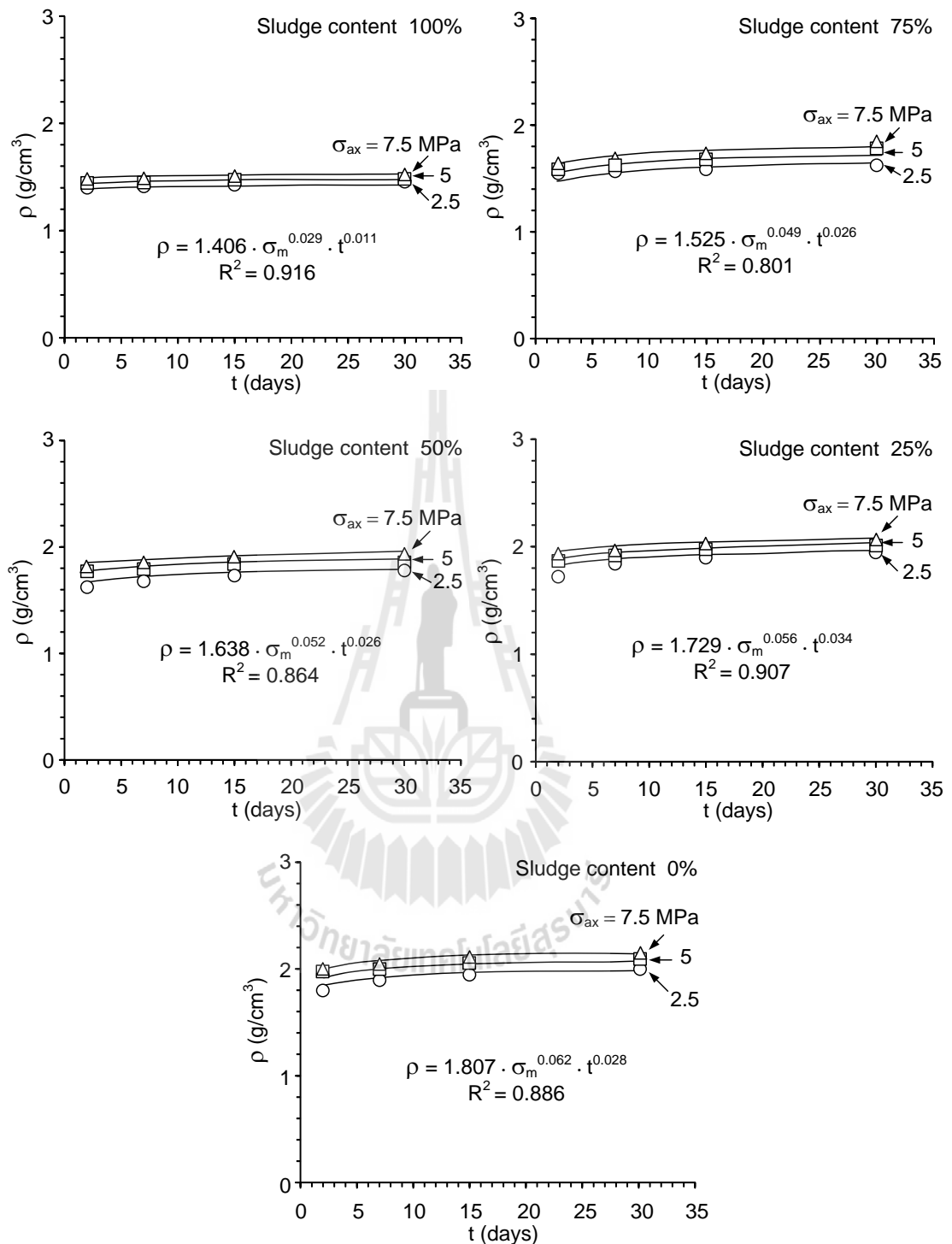


Figure 5.6 Density (ρ) as a function of time (t) and mean stresses (σ_m), test result (points) and back prediction (lines).

5.3.5 Uniaxial compressive strength of sludge-crushed salt mixture

Uniaxial compressive strength of the sludge-crushed salt samples increase with the decreasing sludge content and increase with axial stresses and consolidation time. The relationships can be represented by:

$$\sigma_c = \lambda \cdot \sigma_m^\mu \cdot t^\nu \quad (5.7)$$

where σ_c is uniaxial compressive strength of sludge-crushed salt sample (MPa), σ_m is mean stress (MPa), t is time for consolidation (days), λ , μ and ν are empirical constants. Regression analysis on the test data can determine these constants (Table 5.5). Good correlation ($R^2 = 0.881$ to 0.972) between the proposed equation and the tests is obtained. Figure 5.7 shows the test data with the back prediction of the proposed equation.

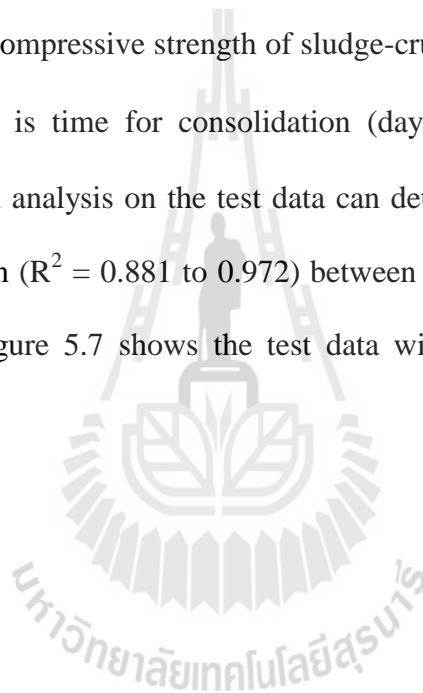


Table 5.5 Parameters of uniaxial compressive strength relationship.

Sludge content by weight (%)	Parameters	Values	Coefficients of correlation
100	λ	0.64	0.931
	μ	0.649	
	ν	0.145	
75	λ	0.715	0.941
	μ	0.713	
	ν	0.16	
50	λ	0.801	0.971
	μ	0.818	
	ν	0.254	
25	λ	0.94	0.972
	μ	0.832	
	ν	0.291	
0	λ	0.971	0.881
	μ	0.84	
	ν	0.344	

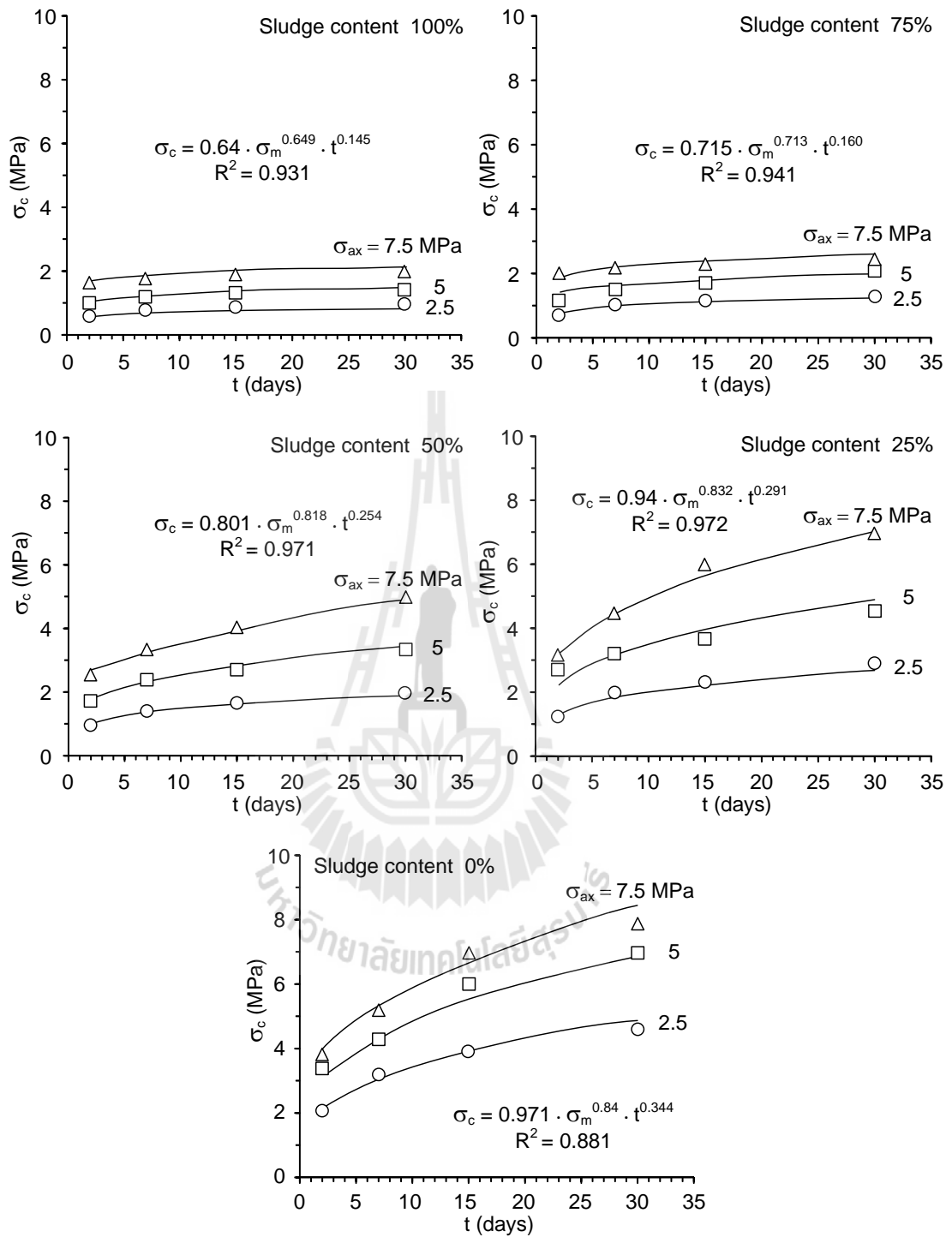


Figure 5.7 Uniaxial compressive strength (σ_c) as a function of time (t) and mean stresses (σ_m), test result (points) and back prediction (lines).

5.3.6 Elastic modulus of sludge-crushed salt mixture

Elastic modulus of the sludge-crushed salt samples increase with the decreasing sludge content and increase with axial stresses and consolidation time. The relationships can be represented by:

$$E = \varepsilon \cdot \sigma_m^\zeta \cdot t^\varpi \quad (5.8)$$

where E is elastic modulus of sludge-crushed salt sample (GPa), σ_m is mean stress (MPa), t is time for consolidation (days), ε , ζ and ϖ are empirical constants. Table 5.6 show constant parameters of elastic modulus relationship. Good correlation is obtained ($R^2 = 0.779$ to 0.958). This equation can be used to predict the intrinsic permeability occurred at consolidation periods and under mean stress. Figure 5.8 shows the test data with the back prediction of the proposed equation.

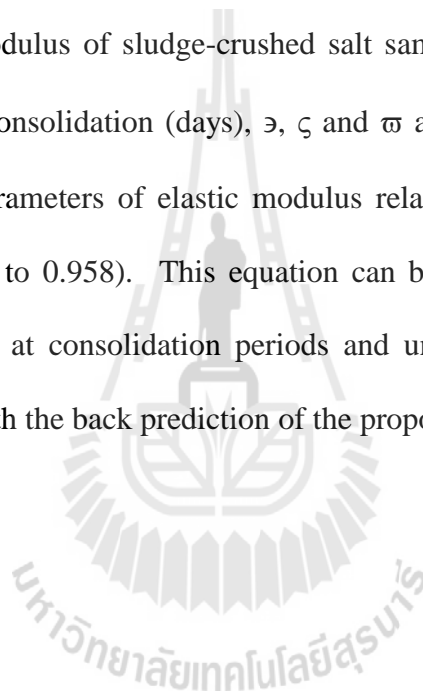


Table 5.6 Parameters of elastic modulus relationship.

Sludge content by weight (%)	Parameters	Values	Coefficients of correlation
100	ϵ	0.064	0.779
	ζ	0.341	
	ω	0.164	
75	ϵ	0.072	0.958
	ζ	0.397	
	ω	0.171	
50	ϵ	0.08	0.941
	ζ	0.487	
	ω	0.182	
25	ϵ	0.086	0.946
	ζ	0.514	
	ω	0.194	
0	ϵ	0.091	0.914
	ζ	0.528	
	ω	0.205	

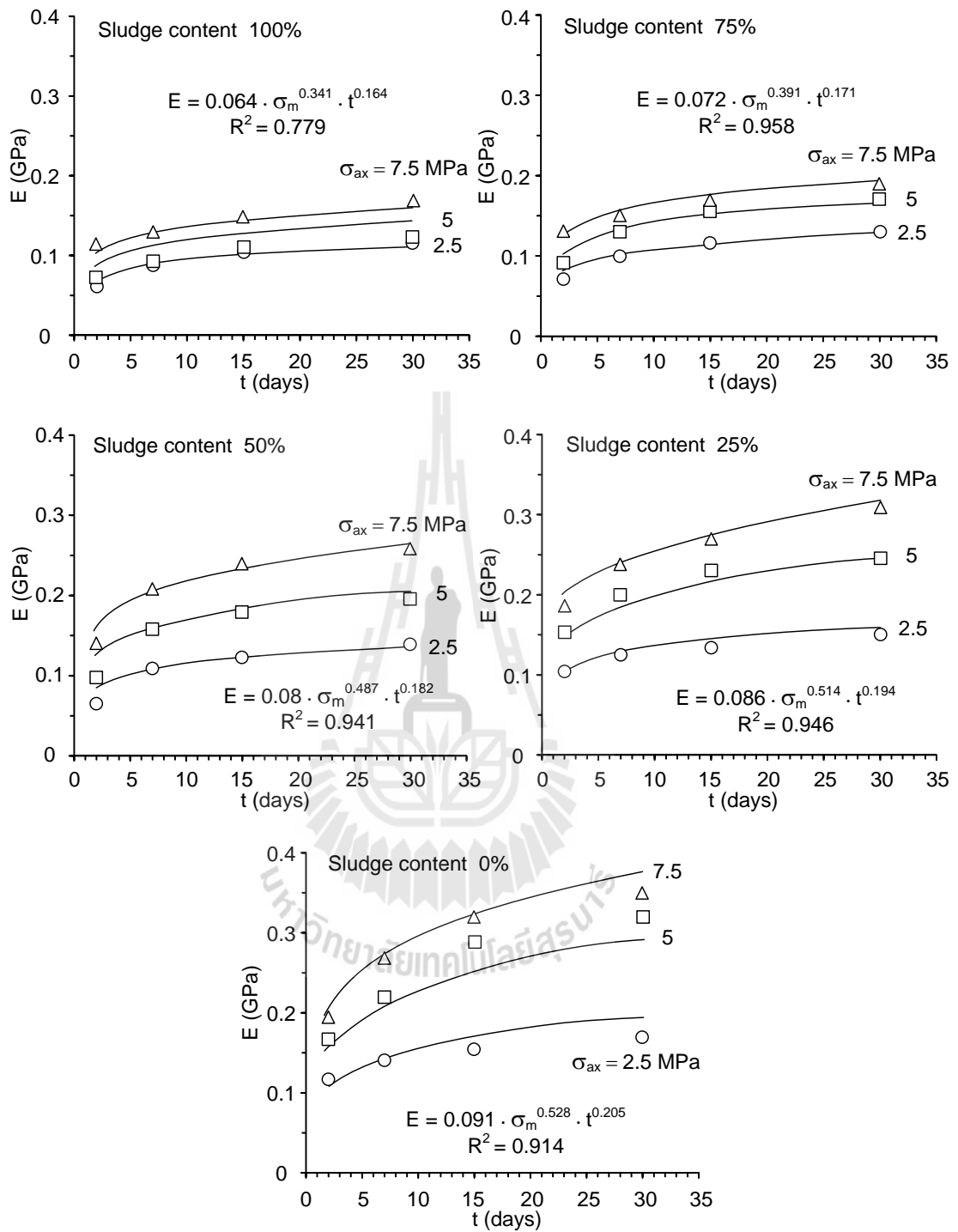


Figure 5.8 Elastic modulus (E) as a function of time (t) and mean stresses (σ_m), test result (points) and back prediction (lines).

5.3.7 Poisson's ratio of sludge-crushed salt mixture

Poisson's ratio of the sludge-crushed salt samples increase with the sludge content, axial stresses and consolidation time. The relationships can be represented by:

$$v = \omega \cdot \sigma_m^\xi \cdot t^\delta \quad (5.9)$$

where v is Poisson's ratio of sludge-crushed salt sample, σ_m is mean stress (MPa), t is time for consolidation (days), ω , ξ and δ are empirical constants. Table 5.7 show constant parameters of Poisson's ratio relationship. Correlation coefficients (R^2) equal to 0.857 to 0.965. This equation can be used to predict the Poisson's ratio occurred at consolidation times and mean stress. Figure 5.9 shows the test data with the back prediction of the proposed equation.

Table 5.7 Parameters of Poisson's ratio modulus relationship.

Sludge content by weight (%)	Parameters	Values	Coefficients of correlation
100	ω	0.166	0.857
	ξ	-0.409	
	∂	-0.300	
75	ω	0.189	0.861
	ξ	-0.354	
	∂	-0.265	
50	ω	0.255	0.965
	ξ	-0.31	
	∂	0.236	
25	ω	0.291	0.953
	ξ	-0.231	
	∂	-0.194	
0	ω	0.317	0.961
	ξ	-0.213	
	∂	-0.139	

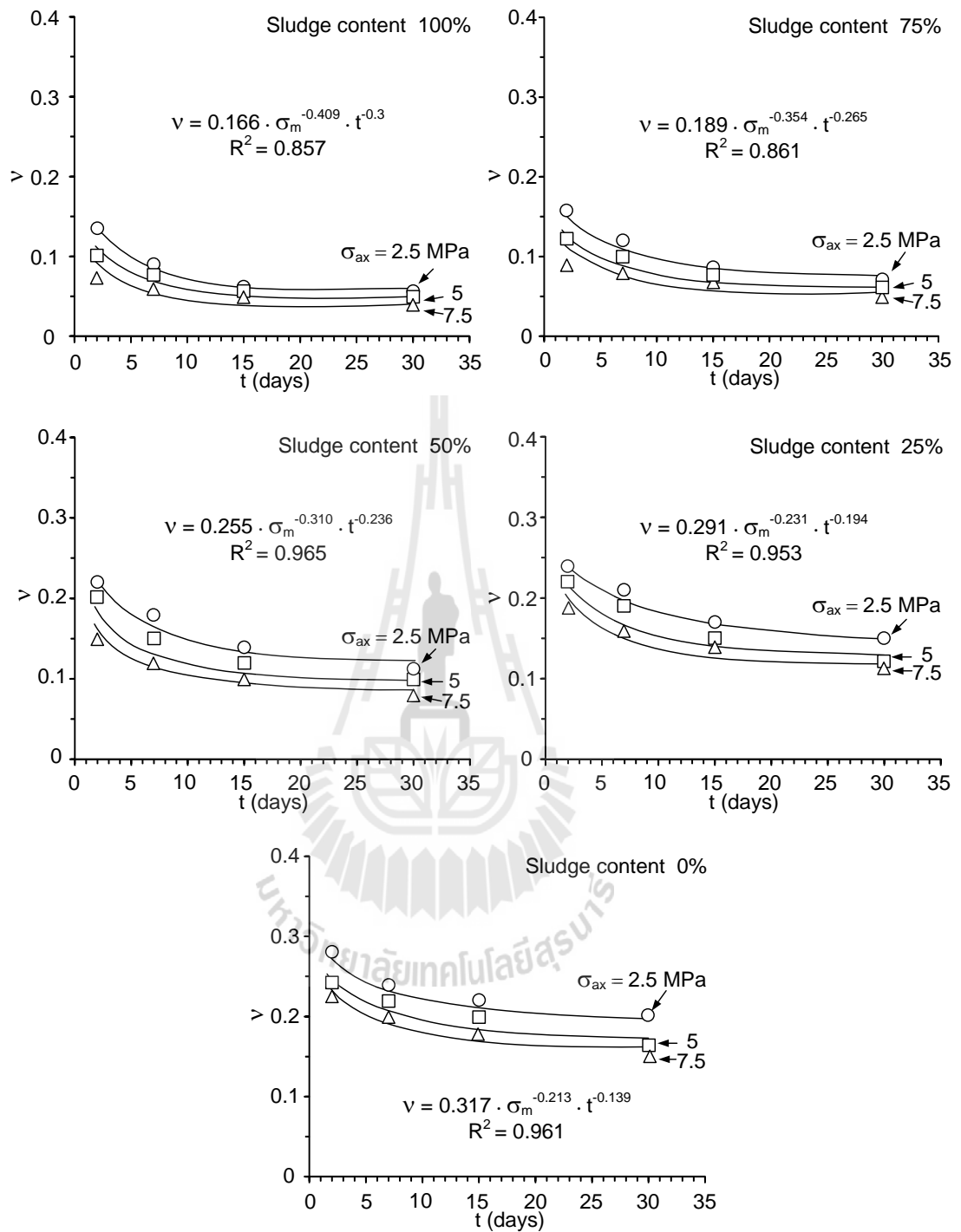


Figure 5.9 Poisson's ratio (ν) as a function of time (t) and mean stresses (σ_m), test result (points) and back prediction (lines).

CHAPTER VII

DISCUSSIONS, CONCLUSIONS AND RECOMMENDATION FOR FUTURES STUDIES

7.1 Discussions

The section discusses the effects of sludge-crushed salt ratios on the mechanical and hydraulic properties for use as backfill material in salt and potash mines and comparisons of the results from this study with those obtained elsewhere under similar test conditions.

- Sludge used here is obtained from Metropolitan Waterworks Authority in Bangkok. The basic properties of the sludge indicate that liquid limit is 59%, plastic limit is 31%, plastic index is 28% and specific gravity 2.56. The sludge sample is classified as silt with over 90% silica of its particles smaller than 0.047 mm. The results obtained here also agree with those of Wetchasat and Fuenkajorn (2013) who study the performance of sludge mixed with the commercial grade Portland cement.
- The results of consolidation test in cylindrical steel tube gives higher axial strain, void ratio and suitable brine than standard size test. The size of cylindrical steel tube used in this study is relatively large as compared to standard size test. Aydilek et al. (1999) study the large-scale and small-scale consolidation tests of wastewater sludge. The specimen of small-scale consolidation tests (ASTM D2435-4) had 50 mm inside diameter and 12 mm height. The large-scale consolidation tests had 50 mm inside diameter and 48 mm height. As a result of the volumetric strains of

large-scale test are much higher than small- scale tests because of high initial water contents and void ratio. This means that the results obtained from this study would give lower volumetric strain than under in-situ installation.

- The volumetric strain of sludge-crushed salt mixture is higher than the pure crushed salt because the sludge-crushed salt mixtures have grain size of sludge is smaller than 0.047 mm. The volumetric strain of the sludge-crushed salt mixtures increases with increasing sludge content and tends to be independent with time. This is because the sludge is classified as elastic silt, cohesionless material, while the volumetric of crushed salt increase with increasing consolidation time due to crushed salt have grain size ranging from 0.075 to 2.35 mm and highly sensitive to time-dependent deformation (Fuenkajorn and Daemen, 1988; Samsri et al., 2010).

- The increasing of sludge content reduces permeability of the mixtures because grain size of sludge is smaller than crushed salt, and hence the mixture can be compacted better than the pure crushed salt. Shor et al. (1981) who conduct the consolidation of crushed salt mixed with brine to study a relationship between permeability, porosity and average initial grain size. They found that the fine grains (0.02 cm) can reduce porosity better than coarse grains (0.34 cm) and the permeability decrease with decreasing porosity.

- The sludge content decreases the uniaxial compressive strength, elastic modulus and Poisson's ratio of the mixtures because sludge is classified as elastic silt with over 90% silica and cohesionless, while crushed salt can deform plasticity under loading, which agrees with Fuenkajorn and Pueakphum (2010) and Samsri et al. (2010).

- Consolidation time of sludge-crushed salt should be longer (month or years) for long-term testing because the mechanical behavior of crushed salt is complex and highly time-dependent deformation as painted by Miao et al. (1995) and Somtong et al. (2013).
- The sludge can be substitute material for bentonite because the similarity of mechanical and hydraulic properties. A comparison between the properties of sludge and bentonite (Daeman and Ran, 1996) is summarized in Table 7.1

Table 7.1 Comparison the properties between sludge and bentonite.

Properties	Material	
	Sludge	Bentonite (Daeman and Ran, 1996)
Composition	Silica 90%	Monmorillonite 90%
Liquid Limite	59	105
Plastic Limit	31	35
Density (g/cm ³)	1.8-2.0	1.8
Permeability (m ²)	Less than 10 ⁻¹¹	Less than 10 ⁻¹⁶
Uniaxial compressive strengths (MPa)	2.0-7.0	2.9-5.0
Swell pressure (MPa)	-	1-2
Brine content (%)	5	4

7.2 Conclusions

All objectives and requirements of this study have been met. The results of the laboratory testing and analyses can be concluded as follows:

- The sludge is classified as elastic silt with over 90% of its particle is smaller than 0.047 mm. The main mineral composition is silica. The basic properties of the sludge indicate that liquid limit is 59%, plastic limit is 31%, plastic index is 28% and specific gravity is 2.56.
- Crushed salt used in this study have been obtained from the Middle member of the Maha Sarakham Formation in the Korat basin, northeastern Thailand. The grains size of crushed salt ranges from 0.075 to 2.35 mm.
- The proportion of saturated brine to sludge-crushed salt mixture in this study is determined as 5% by weight.
- The volumetric strains increase with the sludge content, axial stresses and consolidation time.
- The permeability of sludge-crushed salt mixtures decrease with increasing sludge contents, axial stresses and consolidation time. The outflow of mixtures at 50:50, 75:25 and 100:0 cannot be detected. The lower limit of the measurement system is 10^{-11} m^2 .
- The uniaxial compressive strength, elastic modulus and density of the mixtures increase with the axial stresses and time, and decrease with increasing sludge contents. Poisson's ratios decrease with increasing sludge content, axial stress and time. The lowest compressive strength is observed for sludge content of 100% with consolidation stress = 2.5 MPa at 2 days, which equal to 0.63 MPa. The highest compressive strength is observed for 7.5 MPa consolidation stress of pure crushed salt

which equals 7.9 MPa. The elastic modulus, Poisson's ratios and density are 0.35 GPa, 0.28 and 2.1 g/cm^3 respectively after 30 days of consolidation.

- All test results are used to develop set of empirical equation to predict the mechanical and hydraulic properties of sludge-crushed salt mixture after installation as backfill material in the mine opening.

- The results of computer simulations are evaluated in term of the effectiveness for 50 years by various sludge contents at 25, 50 and 75 % by weight. The results suggest that the deformation of surface subsidence, roof, floor and pillar increase with increasing overburden thickness, opening height and duration before backfill. The surface subsidences of these models increases during the first 10 years after the backfilling emplacement and remains constant through the next 50 years. The lower subsidence observes for sludge = 25% by weight ranging from 3.93 to 7.48 cm. The higher subsidence observes for sludge = 75% by weight ranging from 4.03 to 9.12 cm.

7.3 Potential applications

The section discusses about applications of sludge-crushed salt mixtures for backfill material in salt and potash mines.

- Surface subsidence due to the deformation of pillar and roof of underground mine is a problem of the salt and potash mining. The sludge-crushed salt mixture can use as backfill for reduce deformation of pillar and roof of underground opening. The sludge content can reduce permeability better pure crushed salt. While the sludge content decrease the uniaxial compressive strengths, elastic modulus and Poisson's ratio of the mixtures. The sludge-crushed salt mixture of 25:75 by weight is probably the most suitable for backfill material because their mechanical properties are higher

than the sludge-crushed salt mixtures of 50:50 and 75:20 by weight. The permeability of mixture under consolidation condition for a month is less than 10^{-11} m^2 and is dependent with consolidation time. It can reduce the deformation of room and pillar better than those, and hence the surface subsidence decreases.

- The different mixture between sludge-crushed salt mixtures 25:75 by weight and bentonite-crushed salt mixtures 30:70 by weight (Butcher, 1991; Pfeifle, 1991) are compared in tend of the mechanical and hydraulic properties for backfill. The results of comparison are summarized in Table 7.2. The sludge-crushed salt mixtures have the mechanical and hydraulic properties comparable to those of bentonite-crushed salt mixtures. Therefore, the sludge can use as a substituted material to mix with crushed salt for backfill in salt and potash mines. Such application can also minimize the disposal cost of the sludge and reduce deformation of surface subsidence, pillar and roof of salt and potash mines.

7.4 Recommendations for futures studies

The test results for the sludge-crushed salt mixture have been limited to consolidation stresses and time. To confirm the conclusions drawn in this research, more testing is required as follows:

- Sludge-crushed salts mixture should be performed on a wider range of consolidation periods and consolidation stresses.
- Sludge should be collected from sludge lagoon in various seasons.
- Testing time and curing time should be longer (month or years) for long-term testing.

- Sludge from other plants may be needed to compare the results. The relationship between the temperature, mechanical and hydraulic properties of crushed salt during consolidation should be investigated.

Table 7.2 Comparison of mechanical and hydraulic properties between sludge-crushed salt mixtures 25:75 by weight and bentonite-crushed salt mixtures 30:70 by weight (Butcher, 1991; Pfeifle, 1991).

Properties	Sludge-crushed salt mixtures 25:75 by weight	Bentonite-crushed salt mixtures 30:70 by weight
Permeability (m ²)	Less than 10 ⁻¹¹	Less than 10 ⁻¹⁵
Volumetric strain	200-350	300-350
Uniaxial compressive strength (MPa)	2.0-7.0	1.0-8.1
Density (g/cm ³)	1.8-2.0	1.4-2.0
Swell pressure (MPa)	-	2.3-3.5
Brine content (%)	5	3

REFERENCES

- ASTM D2434-68. Standard test method for Permeability of Granular Soils (Constant Head). In **Annual Book of ASTM Standards**. Philadelphia: American Society for Testing and Materials.
- ASTM D2435-04. Standard test methods for one-dimensional consolidation properties of soils using incremental loading. In **Annual Book of ASTM Standards**. Philadelphia: American Society for Testing and Materials.
- ASTM D2938-95. Standard test method for unconfined compressive strength of intact rock core specimens. In **Annual Book of ASTM Standards**. Philadelphia: American Society for Testing and Materials.
- Aydilek, A.H., Edil, T.B. and Fox, P.J. (1999). Consolidation characteristic of wastewater sludge. **American society for testing and materials**. pp.15.
- Brodsky, N. S., Zeuch, D.H., and Holcomb, D.J. (1995). Consolidation and permeability of crushed salt WIPP salt. In **Proceedings of the Fouth Conference on the Mechanical Behavior of Salt** (pp. 303-316). Clausthal-Zellerfeld, Germany.
- Brodsky, N.S. (1994) Hydrostatic and shear consolidation tests and permeability measurements on Waste Isolation Pilot Plant crushed salt (SAND93-7058). **Sandia national laboratories**. Albuquerque.

- Bunjongsiri, K. and Bunjongsiri, J. (2005). A study of quantity of heavy metal in bricks produce by clay mix with sludge from community wastewater treatment. In **Proceedings of the Eleventh Conference on International Convention on Civil Engineering**. Pattaya, Chonburi.
- Butcher, B.M. (1991) The advantages of a salt/bentonite backfill for Waste isolation pilot plant disposal rooms (Contractor Report SAND90-3074). **Sandia National Laboratories**.
- Callahan, G. D. and Loken, M. C. (1996). Evaluation of constitutive models for crushed salt. In **Proceedings of the Fourth Conference on the Mechanical Behavior of Salt**. Montreal, Canada.
- Case, J.B. and Kelsall, P. (1987). Laboratory investigation of crushes salt consolidation. **International Journal of Rock Mechanics and Mining Science and Geomechanics Abstracts**. 25 (5): 216-223.
- Crosby, K. (2007). Integration of rock mechanics and geology when designing the Udon South sylvinitic mine. In **Proceedings of the First Thailand Symposium on Rock Mechanics** (pp. 3-22). Nakhon Patchasima.
- Daemen, J.J.K. and Ran, C. (1996). Bentonite as a Waste Isolation Pilot Plant Shaft Sealing Material (Contractor Report SAND96-1968). **Sandia National Laboratories**. Albuquerque.
- Fossum, A.F., Callahan, G.D., Van Sambeek, L.L. and Senseny, P.E. (1988). How Should One-Dimensional Laboratory Equations be Cast Into Three-Dimensional. In **Proceedings of the Twenty-ninth U.S. Symposium on Rock Mechanics** (pp. 35-41). University of Minnesota, Minneapolis, Rotterdam.

- Fuenkajorn, K. and Daemen, J. J. K. (1988). Boreholes closure in salt. **Technical Report Prepared for The U.S. Nuclear Regulatory Commission** (Report No. NUREG/CR-5243 RW). University of Arizona.
- Fuenkajorn, K. and Phueakphum, D. (2010). Effects of cyclic loading on mechanical properties of Maha Sarakham salt. **Engineering Geology**. 112 (1-4) 43-52.
- Hansen, F. D. (1997). Reconsolidating salt: compaction constitutive modeling, and physical processes. **International Journal of Rock Mechanics and Mining Sciences**. 34: 3-4.
- Hansen, F. D. and Mellegard, K. D. (2002). Mechanical and permeability properties of crushed salt. In **Proceedings of the Fifth Conference on the Mechanical Behavior of Salt** (pp. 253-256). Bucharest, Romania.
- Hein, H.J. (1991). **Ein Stoffgesetz zur Beschreibung desthermomechanischen Verhaltens von Salzgranulat**. Thesis Technical University Aachen.
- Indraratna, B., and Ranjith, P. (2001). **Hydromechanical aspect and unsaturated flow in joints rock**. A. A. Balkema, Lisse. pp. 83-154.
- ISRM (1987). Suggested method for determining deformability of rock materials in uniaxial compression. In **Brown ET (ed) international society for rock mechanics suggested methods**.
- Itasca (1992) **User manual for FLAC-fast Lagrangian analysis of continua, version 3.0**. Itasca Consulting Group Inc., Minneapolis, MN.
- Jaeger, J.C, Cook, N.G.W., Zimmerman, R.W. (2007). **Fundamental of Rock Mechanics** (Fourth edition). Blackwell Publishing, Australia. pp. 475.
- Japakasetr, T. and Suwanich, P. (1977). Potash and rock salt in Thailand Bangkok: Economic Geology Division. **Department of Mineral Resources**. Bangkok.

- Japaksetr, T. (1985). Review on rock salt and potash exploration in Northeast Thailand. In **Proceedings Conference on Geology and Mineral Resources Development of the Northeast of Thailand** (pp. 135-147). Khon Kaen University, Thailand.
- Kelsall, P.C., Case, J.B., Coons, W.E., Franzone, J.G. and Meyer, D. (1984). Schematic designs for penetration seals for a repository in the Permian basin. WMI/ONWI-564, prepared by IT Corporation for office of Nuclear Waste Isolation. **Battelle Memorial Institute**. Columbus, Ohio.
- Kongthong, R. and Lertpocasombut, K. (2006). A study of sludge from water treatment plant on dye adsorption. In **Proceedings of the Eleventh Conference on International Convention on Civil Engineering**. Phuket.
- Laothong, K. (2003). **The Utilization of Sludge Cake from Water Treatment Processes of Wang Noi Power Plant**. Master of Engineering (Environmental Engineering), Major Field Environmental Engineering, Department of Environmental Engineering, Kasetsart University. pp. 99.
- Loken, M.C. and Statham, W. (1997). Calculation of density and permeability of compacted crush salt within an engineered shaft sealing system. **Computer in Civill Engineering**. pp. 485-492.
- Miao, S., Wang, M.L. and Schreyer, H.L. (1995). Constitutive models for healing of materials with application to compaction of crushed rock salt. **Engineering mechanics**. 121 (10): 1122-1129.
- O'Kelly (2004). Mechanical properties of dewatered sewage sludge. **Waste management**. 24: 47-52.

- Pfeifle, T.W. (1991). Consolidation, permeability, and strength of crushed salt/bentonite mixtures with application to the WIPP (Contractor Report SAND90-7009). **Sandia National Laboratories**.
- Poonsawat, C. and Lertpocasombut, K. (2006). Study on the properties of sludge from water supply plant as raw material for clay plan roofing tile. In **Proceedings of the Eleventh Conference on International Convention on Civil Engineering**. Phuket.
- Pudewills, A. and Krauss, M. (1999). Implementation of a viscoplastic model for crushed salt in the ADINA program. **Computer and Structure**. 72 (1-3): 293-299
- Ran, C. and Daemen, J.J.K. (1995). The influence of crushed salt particle gradation on compaction. In **Proceedings of The Thirty-fifth U.S. Symposium on Rock Mechanics** (pp.761-766). Reno, NV, A.A. Balkema, Rotterdam.
- Samsri, P., Sriapai, T., Walsri, C. and Fuenkajorn, K. (2010). Polyaxial creep testing of rock salt. In **Proceedings of the Third Thailand Symposium on Rock Mechanicson** (pp. 125-132). Thailand.
- Sangiumsak, N. and Cheerarot, R. (2008). The study of properties of artificial aggregates made from water supply sludge. In **Proceedings of the Eleventh Conference on International Convention on Civil Engineering**. Pattaya, Chonburi.
- Shor, A.J., Baes, C.F. and Canonico, C.M. (1981). Consolidation and permeability of salt in brine (ORNL-5774). **The Oak Ridge National Laboratory for the U.S. Department of Energy**. Oak Ridge, TN.

- Somtong, S., Tepnarong, P. and Fuenkajorn, K. (2013). Strength and permeability of consolidated crushed salt. In **Proceedings of the EIT-JSCE International Symposium on International Human Resource Development for Disaster-Resilient Countries**. September 12-13, Imperial Queen's Park Hotel, Bangkok, Thailand.
- Sriapai. T., Chaowarin, W. and Fuenkajorn, K. (2012). Effects of temperature on compressive and tensile strengths of salt. **Science Asia**. 38: 166-174.
- Stormont, J.C. and Finley, R.E. (1996). Sealing borehole in rock salt. **Sealing of Boreholes and Underground Excavations in Rock** (K. Fuenkajorn and J.J.K. Daemen eds) (pp.184-224). Chapman and Hall, London.
- Suriyachat, D., Vichitamornpun, P. and Ruengsumrej, W. (2004). Water treatment sludge utilization (Technical Report No. 16/2547). **Department of primary industries and mines**. Bangkok.
- Suwanich, P. and Ratanajaruraks, P. (1986). Sequences of rock salt and potash in Thailand (Nonmetallic Minerals Bulletin No. 1). Bangkok: Economic Geology, Division. **Department of Mineral Resources**. Bangkok.
- Suwanich, P., Ratanajaruraks, P. and Kunawat, P. (1982). Core log Bamnet Narong area at Chaiyaphum province. Bangkok: Economic Geology Division. **Department of Mineral Resources**. Bangkok.
- Valls, S., Yague, A., Vazque, E. and Mariscal, C. (2004). Physical and mechanical properties of concrete with added dry sludge from a sewage treatment plant. **Cement and Concrete Research**. 34: 2203-2208.

- Van Impe, P.O. Barbetti, L. and Van Impe W.F. (2009). Determination of consolidation parameters of dredging and industrial waste sludge. In **Proceedings of the International Symposium on Engineering Practice and Performance of Soft Deposits**. Osaka, Japan.
- Wagner, R.A. Callahan, G. D. and Butcher, B. M. (1990). Mechanical analyses of WIPP disposal rooms backfilled with either crushed salt or crushed salt-bentonite. In **Proceedings on Materials Research Society**. 207: 169-175
- Wendai, L. (2000). **Regression analysis, linear regression and probit regression in 13 chapter**. SPSS for Windows: statistical analysis, Publishing House of Electronics Industry, Beijing.
- Wetchasat, K. and Fuenkajorn, K., (2013). Laboratory Assessment of Mechanical and Hydraulic Performance of Sludge-Mixed Cement Grout in Rock Fractures. In **Proceedings of the Fourth Thailand Symposium on Rock Mechanics**. Wang Nam Keaw, Nakhon Ratchasima, Thailand.
- Zeuch, D.H. (1990). Isostatic hot pressing mechanism maps for pure and natural sodium chloride: applications to nuclear waste Isolation in bedded and domal salt formations. **Rock mechanical and mineral sciences and geomechanical**. 27: 505-524.

BIOGRAPHY

Mr. Adison Bumrungsuk was born on January 21, 1990 in Bangkok province, Thailand. He received his Bachelor's Degree in Science (Geoscience) from Mahidol University in 2012. For his post-graduate, he continued to study with a Master's degree in the Geological Engineering Program, Institute of Engineering, Suranaree university of Technology. During graduation, 2014-2016, he was a part time worker in position of research assistant at the Geomechanics Research Unit, Institute of Engineering, Suranaree University of Technology. He published technical paper related to rock mechanics, titled mechanical and hydraulic properties of sludge-crushed salt mixture as applied for backfill material in salt and potash mines in the Proceeding of the 9th South East Asia Technical University Consortium (SEATUC) Symposium 2015, Suranaree University of Technology, Nakhon Ratchasima, Thailand.